



Modeling uncertainties for tropospheric nitrogen dioxide columns affecting satellite-based inverse modeling of nitrogen oxides emissions

J.-T. Lin¹, Z. Liu², Q. Zhang³, H. Liu⁴, J. Mao^{5,6}, and G. Zhuang⁷

¹Laboratory for Climate and Ocean-Atmosphere Studies, Department of Atmospheric and Oceanic Sciences, School of Physics, Peking University, Beijing 100871, China

²Combustion research facility, Sandia National Laboratories, Livermore, CA 94551, USA

³Center for Earth System Science, Tsinghua University, Beijing, China

⁴National Institute of Aerospace, Hampton, VA 23666, USA

⁵Program in Atmospheric and Oceanic Sciences, Princeton University, Princeton, NJ 08542, USA

⁶Geophysical Fluid Dynamics Laboratory/National Oceanic and Atmospheric Administration, Princeton, NJ 08542, USA

⁷Center for Atmospheric Chemistry Study, Department of Environmental Science and Engineering, Fudan University, Shanghai, 200433, China

Correspondence to: J.-T. Lin (linjt@pku.edu.cn)

Received: 22 April 2012 – Published in Atmos. Chem. Phys. Discuss.: 7 June 2012

Revised: 5 November 2012 – Accepted: 3 December 2012 – Published: 21 December 2012

Abstract. Errors in chemical transport models (CTMs) interpreting the relation between space-retrieved tropospheric column densities of nitrogen dioxide (NO₂) and emissions of nitrogen oxides (NO_x) have important consequences on the inverse modeling. They are however difficult to quantify due to lack of adequate in situ measurements, particularly over China and other developing countries. This study proposes an alternate approach for model evaluation over East China, by analyzing the sensitivity of modeled NO₂ columns to errors in meteorological and chemical parameters/processes important to the nitrogen abundance. As a demonstration, it evaluates the nested version of GEOS-Chem driven by the GEOS-5 meteorology and the INTEX-B anthropogenic emissions and used with retrievals from the Ozone Monitoring Instrument (OMI) to constrain emissions of NO_x. The CTM has been used extensively for such applications. Errors are examined for a comprehensive set of meteorological and chemical parameters using measurements and/or uncertainty analysis based on current knowledge. Results are exploited then for sensitivity simulations perturbing the respective parameters, as the basis of the following post-model linearized and localized first-order modification. It is found that the model meteorology likely contains errors of various magnitudes in cloud

optical depth, air temperature, water vapor, boundary layer height and many other parameters. Model errors also exist in gaseous and heterogeneous reactions, aerosol optical properties and emissions of non-nitrogen species affecting the nitrogen chemistry. Modifications accounting for quantified errors in 10 selected parameters increase the NO₂ columns in most areas with an average positive impact of 18 % in July and 8 % in January, the most important factor being modified uptake of the hydroperoxyl radical (HO₂) on aerosols. This suggests a possible systematic model bias such that the top-down emissions will be overestimated by the same magnitude if the model is used for emission inversion without corrections. The modifications however cannot eliminate the large model underestimates in cities and other extremely polluted areas (particularly in the north) as compared to satellite retrievals, likely pointing to underestimates of the a priori emission inventory in these places with important implications for understanding of atmospheric chemistry and air quality. Note that these modifications are simplified and should be interpreted with caution for error apportionment.

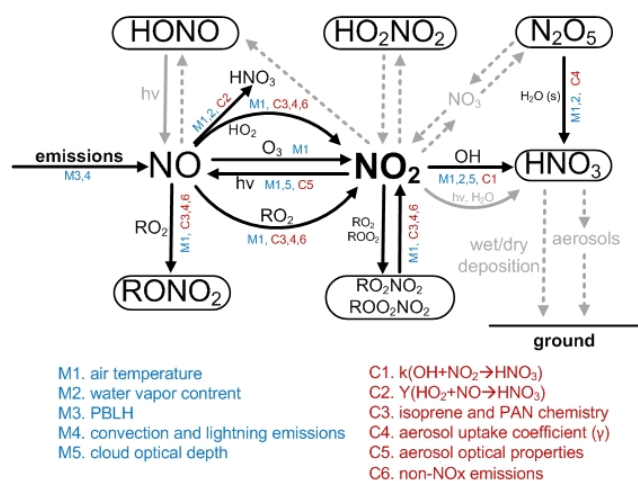


Fig. 1. Tropospheric chemistry involving NO_x and impacts of meteorological and chemical parameters evaluated in the present study. Processes shown in solid grey arrows are discussed without sensitivity simulations. Processes shown in dashed grey arrows are not discussed explicitly. Note that PBL mixing and convection affect vertical distributions of NO_x and related species. Heterogeneous uptake on aerosols depends on the amount of aerosol surfaces as well. Evaluation on the RONO₂ pathway is focused mainly on isoprene nitrates. Clouds and water vapor have indirect influences on radicals through effects on solar radiation.

1 Introduction

Anthropogenic emissions of nitrogen oxides (NO_x ≡ NO + NO₂) in China have been growing at an average rate of about 8 % per year (e.g., Richter et al., 2005; Lin and McElroy, 2011) over the past decade, disrupted temporarily by various socioeconomic events such as the economic downturn, the Olympics and Chinese New Year (Mijling et al., 2009; Lin et al., 2010a; Lin and McElroy, 2011). The rising emissions have attracted tremendous attention concerning the consequences on tropospheric chemistry, air pollution, climate forcing and acid deposition over both source and downwind regions (e.g., Streets et al., 2003; Richter et al., 2005; Martin et al., 2006; Stavrou et al., 2008; Lin et al., 2010a; Lin, 2012; Zhang et al., 2007).

Once emitted into the troposphere, NO_x undergo various sink processes including formation of nitric acid via gaseous and heterogeneous reactions and formation of organic nitrates (peroxyacyl nitrates, alkyl nitrates, etc.) (Fig. 1). These processes are simulated by chemical transport models (CTMs) to constrain emissions and variability of NO_x from the top-down perspective, utilizing space-based measurements of vertical column densities of tropospheric nitrogen dioxide (NO₂) (e.g., Jaeglé et al., 2005; van der A et al., 2006; Lin, 2012). The top-down constraint is a useful supplement to bottom-up estimates, which are subject to uncertainties in emission factors and emission activities (Streets et al., 2003; Zhang et al., 2009b). It is however affected by errors

not just in satellite retrievals but also in CTMs simulating the fate of nitrogen emitted into the troposphere (Martin et al., 2006; Lin et al., 2010b). Errors in model simulations are estimated often from ground-based and aircraft measurements of nitrogen, mostly in a short time period, over the developed countries or over remote/downwind regions (e.g., Hudman et al., 2007; Brinkma et al., 2008; Boersma et al., 2009; Lamsal et al., 2010; Lin and McElroy, 2010). Conclusions drawn are adopted for China and other countries/regions where in situ measurements are not available (e.g., Martin et al., 2006; Zhao and Wang, 2009; Lin et al., 2010b). However, the magnitude and causes of model errors may be region and time dependent, resulting in uncertainties in the applicability of findings from model evaluation limited in time and space. For example, errors in model meteorology may depend on locations and seasons; errors in heterogeneous reactions on aerosol surfaces are important mainly at locations with high aerosol loadings (see Sects. 4 and 5). Even for areas with nitrogen observations, it is still difficult to evaluate the model capability in relating emissions and atmospheric abundances based on measured nitrogen concentrations alone without accurate information on emissions. Lin and McElroy (2010) evaluated the modeled vertical mixing in the planetary boundary layer (PBL) over the northeast US using aircraft observations. They noted that modeled concentrations of NO₂ are much lower than observed values throughout the PBL, which may or may not be caused entirely by emission errors.

The present study proposes an alternate approach for model evaluation over China, by analyzing the sensitivity of simulated NO₂ columns to model meteorological and chemical parameters of importance to the nitrogen chemistry (Fig. 1). A large number of sensitivity simulations are conducted to evaluate the impacts of errors in model meteorological fields constrained by ground- and space-based measurements. The model chemistry is evaluated with additional simulations addressing the embedded errors/uncertainties based on current understanding. Improvements on the estimate of NO₂ columns are achieved then by linearized and localized first-order modifications accounting for quantified errors in model meteorological and chemical parameters. The method is useful for China due particularly to lack of adequate and timely measurements of nitrogen constituents for more direct model evaluation.

As a demonstration, this study evaluates tropospheric NO₂ columns simulated by the nested GEOS-Chem model (Chen et al., 2009) in use of inferring emissions of NO_x from NO₂ columns retrieved from the Ozone Monitoring Instrument (OMI). GEOS-Chem has been used extensively for such top-down constraints over a variety of temporal and spatial scales (Jaeglé et al., 2005; Martin et al., 2006; Boersma et al., 2008; Zhang et al., 2008; Lin et al., 2010b; Lamsal et al., 2011; Lin and McElroy, 2011; Lin, 2012; Wang et al., 2012). Findings from the analysis of GEOS-chem simulations may be applicable to some extent to other models with different meteorological data and/or chemical schemes. The analysis is

focused in East China (101.25–126.25° E, 19–46° N) concerning the extensive inverse modeling studies addressing its significant and rapidly increasing emissions of NO_x in recent years (e.g., Richter et al., 2005; Lin, 2012). Simulations for January and July 2006 are both evaluated to account for potential seasonal dependence of model errors.

The remaining sections are organized as follows. Section 2 presents meteorological observations from the ground networks and satellite remote sensing, as well as space-based measurements of aerosol optical depth (AOD) and NO₂ columns. Section 3 presents the CTM simulations and a brief comparison with satellite retrievals. Sections 4 and 5 evaluate the impacts on simulated NO₂ columns of potential errors in model meteorological and chemical parameters, respectively, by employing a large set of sensitivity simulations. The test simulations are conducted based on current understanding of the nitrogen chemistry, as shown in Fig. 1. Section 6 makes an attempt to modify the simulated NO₂ columns on the first order accounting for quantified errors in model meteorology and chemistry. Section 7 summarizes the present study.

2 Ground and space measurements

2.1 Meteorological observations

Ground measurements for January and July 2006 are taken from the National Oceanic and Atmospheric Administration (NOAA) National Climatic Data Center (NCDC) Integrated Surface Hourly (ISH) dataset (DS3505) for a variety of meteorological parameters, including air temperature, relative humidity (RH), surface air pressure, wind speed at 10 m, and precipitation. The ISH dataset combines measurements from various networks publicly available for weather and climate analyses. It was used by Lin and McElroy (2011) to analyze the day-to-day variation of meteorology in January 2009 of relevance to changes in NO₂ columns retrieved from space and simulated by GEOS-Chem. Here meteorological data are taken from a total of 284 stations across East China. They are available every 3 h (starting from 00:00 UTC) with the exception of daily precipitation data.

Space measurements of tropospheric water vapor path, cloud fraction and cloud optical depth (COD) are taken from the International Satellite Cloud Climatology Project (ISCCP) D2 dataset. The ISCCP dataset is used widely in studies of clouds and the hydrological cycle. It provides monthly mean data on the 2.5° long × 2.5° lat grid for time of day from 00:00 to 21:00 UTC at 3-h intervals for cloud fraction and COD, and monthly mean daily mean data for water vapor path. Here data for January and July 2006 are sampled at the locations of ground meteorological stations for comparison with the GEOS-5 meteorology.

The vertical gradient of meteorological parameters is also important for chemical simulations. For example, vertical gradients of air temperature, water vapor and winds affect the

stability of the PBL (Holtslag and Boville, 1993) and mixing of pollutants with consequences on the chemical and deposition processes (Lin and McElroy, 2010, 2011). However, no data are available to allow for systematic evaluation of errors in vertical profiles of model meteorological parameters. Further research is needed to explore this issue.

2.2 NO₂ columns from OMI

Onboard the Aura satellite, OMI flies over China at around 01:30 LT in the afternoon. Retrievals of OMI NO₂ columns are taken from the DOMINO product version 2 (Boersma et al., 2011). The processing of DOMINO-2 is presented in Lin (2012), including but not limited to the conversion from level 2 to level 3 monthly data and an analysis of retrieval errors. Level-2 data are chosen from snow-ice cloud-free (cloud radiance fraction ≤ 50 %) pixels. Of the 60 pixels from each scan, only 30 pixels with the smallest viewing zenith angles (cross-track length ≤ 30 km) are used; this corresponds to an effective swath of about 800 km and a global coverage every three days. The level 3 data are derived on the 0.25° long × 0.25° lat grid for January and July 2006.

2.3 MODIS AOD

To evaluate modeled optical properties of aerosols, measurements of aerosol optical depth (AOD) at 550 nm are taken from the MODIS/Aqua level 2 collection 5.1 product. Data for January and July 2006 are sampled at the locations of ground meteorological stations for comparison with GEOS-Chem simulations. For a given station, MODIS data for each day available within 0.25° of the station are averaged to obtain the daily value.

3 GEOS-Chem simulation and comparison with OMI retrievals

This study evaluates the nested model for Asia (Chen et al., 2009) of GEOS-Chem (version 8-03-02; <http://wiki.seas.harvard.edu/geos-chem/index.php/MainPage>). The model is driven by the assimilated meteorological fields of GEOS-5 taken from the National Aeronautics and Space Administration (NASA) Global Modeling and Assimilation Office (GMAO). It is run with the full O_x-NO_x-CO-VOC-HO_x chemistry and online calculation for various aerosols (sulfate, nitrate, ammonium, black carbon, primary organic carbon, sea salt and dust). The nested model has a horizontal resolution of 0.667° long × 0.5° lat with 47 vertical layers; each of the lowest 10 layers is about 130 m thick. Its lateral boundary conditions are updated every 3 h from a respective global simulation at 5° long × 4° lat. Another model setup is detailed in Lin (2012), including emissions and their temporal variability. In particular, anthropogenic emissions in Asia are taken from the INTEX-B inventory as representative of 2006 (Zhang et al., 2009b) for various species including NO_x,

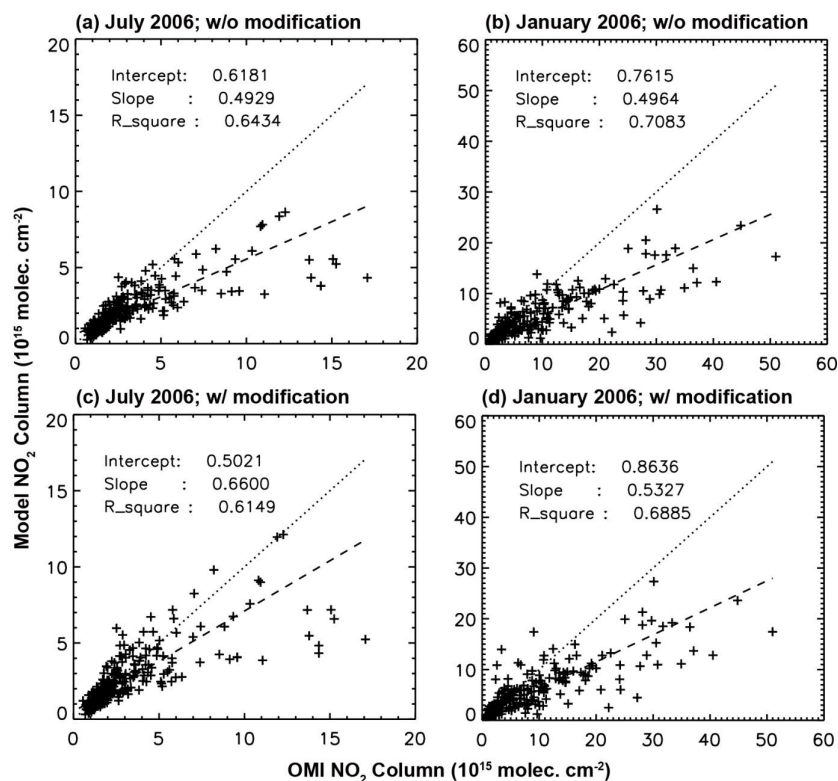


Fig. 2. Scatter plot for NO_2 columns at the 284 meteorological stations in East China retrieved from OMI and simulated by GEOS-Chem with and without post-model modifications discussed in Sect. 6. Also presented is the statistics from the RMA regression.

carbon monoxide (CO), non-methane volatile organic compounds (VOCs), sulfur dioxide (SO_2), black carbon (BC) and primary organic carbon (OC).

For all simulations (see Table 1), modeled vertical distribution of NO_2 for each day is sampled at the time with valid retrievals, regridded to 0.25° long \times 0.25° lat, and applied with the averaging kernel (AK) from DOMINO-2. The daily data are averaged then to obtain monthly mean values in January and July 2006 for the present analysis.

NO_2 columns derived from the base simulation (Case 1 in Table 1) are compared in detail to retrieved values by Lin (2012). Averaged over East China, model NO_2 columns are lower than the retrievals by about 20% in July and by 36% in January. The underestimate is much more significant in extremely polluted areas such as cities and locations with large point sources, particularly in the north in January: model values are only about 20–30% of retrievals. Results are similar from the comparison at the 284 meteorological stations showing a slope of about 0.5 in both months under the reduced major axis (RMA) regression (Fig. 2a, b). Lin (2012) found that total anthropogenic emissions of NO_x in East China inferred from DOMINO-2 are larger than the INTEX-B inventory by about 40%. These differences are attributable in part to errors in model simulations, as analyzed in the following sections.

4 Sensitivity of GEOS-Chem simulated NO_2 columns to meteorological parameters

Errors in the GEOS-5 meteorological fields have consequences on a variety of atmospheric processes affecting the abundance of tropospheric NO_2 simulated by GEOS-Chem. The GEOS-5 meteorology is evaluated in the Supplement with Figs. S1–S8 using observational data from ISH and IS-CCP. Parameters analyzed include air temperature, RH, tropospheric water vapor path, air pressure, wind speed, cloud fraction, COD and precipitation. The analysis is emphasized in the daytime, particularly at mid-day when the lifetime of NO_x is shortest and has the largest impact on its abundance at the overpass time of OMI (i.e., in the early afternoon). Note that many of the meteorological errors found here are rooted in currently limited understanding of the atmospheric dynamics and physics (e.g., convection and cloud microphysics); therefore the analysis for GEOS-5 has implications for other assimilated/modeled meteorological datasets used to drive chemical transport modeling.

In this section, sensitivity simulations are conducted to evaluate the impacts of errors in air temperature, water vapor content and COD on modeled NO_2 columns, by adjusting the respective parameters in GEOS-Chem (see Fig. 1 and Table 1). Also analyzed are the impacts of potential errors in

Table 1. Sensitivity simulations by adjusting model meteorological or chemical parameters¹.

Case	Parameter	Adjustments	Notes and references
1	Base simulation	No changes in parameters	As in Lin (2012)
2	Air temperature in the lowest 10 layers (about 0–1.3 km)	Decreased by 2 °C in the daytime and increased by 1 °C at night	Based on ISH data
3 ²	Air temperature in the lowest 10 layers (about 0–1.3 km)	Decreased by 5 °C in the daytime and increased by 1 °C at night	Based on ISH data
4	Air temperature in the lowest four layers (about 0–0.5 km)	Decreased by 5 °C in the daytime and increased by 1 °C at night	Based on ISH data
5	Air temperature in the lowest 10 layers (about 0–1.3 km)	Increased by 5 °C at night	Based on ISH data
6	Tropospheric water vapor content	Scaled up by 130 %	Based on ISCCP data
7 ²	Tropospheric water vapor content	Scaled down by 130 %	Based on ISCCP data
8	Cloud optical depth	Assumed to be zero	Based on ISCCP data
9	Cloud optical depth	Decreased by 50 %	Based on ISCCP data
10	Cloud optical depth	Increased by 50 %	Based on ISCCP data
11 ²	Cloud optical depth	Increased by 100 %	Based on ISCCP data
12	Cloud optical depth	Evenly distributed in all tropospheric layers	Based on ISCCP data and Liu et al. (2009)
13	PBLH	Derived online	
14	PBLH	Decreased by 10 % in the daytime and tripled at night	Based on ISH temperature data and Liu et al. (2010)
15	PBLH	Tripled at night	Based on ISH temperature data and Liu et al. (2010)
16	PBLH	PBLH taken from GEOS-4	
17	PBLH	Scaled up by 130 %	To analyze potential causes of underestimated NO ₂ columns
18	PBLH	Scaled up by 200 %	To analyze potential causes of underestimated NO ₂ columns
19 ²	Rate constant for OH + NO ₂ reaction	Scaled down by 130 %	Mollner et al. (2010); Sander et al. (2011)
20	Rate constant for OH + NO ₂ reaction	Scaled up by 130 %	Mollner et al. (2010); Sander et al. (2011)
21	Yield of HNO ₃ from NO + HO ₂ reaction	Assumed to be 5 %	Butkovskaya et al. (2005, 2007, 2009); Sander et al. (2011)
22	Yield of HNO ₃ from NO + HO ₂ reaction	Assumed to be 1 %	Butkovskaya et al. (2005, 2007, 2009); Sander et al. (2011)
23 ²	OH regeneration from isoprene chemistry	Yield of 100 % from isoprene + OH reaction assumed	Butler et al. (2008); Lelieveld et al. (2008); Kubistin et al. (2010)
24	OH regeneration from isoprene chemistry	Isoprene + OH reaction turned off	Kubistin et al. (2010)
25 ²	Net yield of isoprene nitrates	Decreased from 10 to 2.4 %	See review by Paulot et al. (2009). Transport of isoprene nitrates is neglected.
26	Equilibrium constant of PAN	Decreased by 20 %	Sander et al. (2011)
27 ²	Uptake rate of HO ₂ on aerosols	Set at 0.2	Thornton et al. (2008); Jacob (2000); He et al. (2001); Yang et al. (2011)
28	Uptake rate of HO ₂ on sulfate-nitrate-ammonium aerosols in the continental PBL	Set at 0.2	Thornton et al. (2008); Jacob (2000); He et al. (2001); Yang et al. (2011)
29 ²	Uptake rate of N ₂ O ₅ on aerosols	Scaled down by a factor of 10	Bertram et al. (2009); Brown et al. (2009)
30 ²	Aerosol scattering and absorption	Turned off for all aerosols	Based on comparison with MODIS AOD
31	Aerosol scattering and absorption	Turned off for BC alone	Based on comparison with MODIS AOD
32	Emissions of CO and SO ₂	Increased by 50 %	Following Lin et al. (2010b)
33	Emissions of propene	Increased by 50 %	To represent effects of aromatics based on INTEX-B inventory (Zhang et al., 2009b)
34 ²	Emissions of propene	Increased by 300 %	To represent effects of aromatics based on top-down constraint (Liu et al., 2010, 2011)
35	Emissions of CO, SO ₂ and VOC	Increased by 50 %	Following Lin et al. (2010b)

¹ Analyses are done in Sects. 4 and 5 also for other parameters without conducting additional sensitivity simulations.² These cases are used for post-model modifications described in Table 2 and analyzed in Sects. 6 and 7.

convection (and resulting lightning emissions of NO_x) and vertical mixing in the PBL.

Errors in RH affect wet deposition of various species and hygroscopic growth of aerosols. These factors are accounted for implicitly with adjusted air temperature and water vapor as the CTM re-calculates RH during the simulation (instead of using RH outputted from GEOS-5). Impacts of errors in 10-m wind speed on modeled NO_2 columns are mainly on the local scale due to the relatively short lifetime of NO_x . Also, biases in wind speed are likely limited to altitudes close to the ground where small-scale variability is not captured by GEOS-5, as expected for an assimilation product (Pryor and Barthelmie, 2011). At higher altitudes, wind speed is better constrained, since the large-scale circulation is reasonably reproduced by GEOS-5 (as suggested by the evaluation for surface air pressure in the Supplement). Errors in precipitation are small on average over East China (see Supplement). Therefore the impacts of these parameters on modeled NO_2 columns are not evaluated explicitly in the present study.

4.1 Air temperature

Errors in air temperature affect the calculation of gaseous and heterogeneous reactions, deposition and biogenic emissions of volatile organic compounds (VOCs), with consequences on modeled NO_2 columns. Their overall impact is evaluated here by sensitivity simulations perturbing air temperature in GEOS-5 (Cases 2–5 in Table 1), based on analysis of temperature in the Supplement.

The first simulation increases the nighttime temperature by 1°C and decreases the daytime temperature by 2°C in the lowest 10 model layers (about 0–1.3 km above the ground) (Case 2 in Table 1). The adjustment extends to the lower troposphere to account for potential errors that may be transported from near the ground to the entire PBL. It also affects the ground temperature, with consequences on modeled biogenic emissions, as well as RH (which is calculated online by the CTM). As a result, modeled NO_2 columns in July are reduced by 0–4 % over most regions with enhancements by up to 10 % over parts of the southwest (Fig. S9a). This is mainly a result of enhanced formation of nitric acid (through enhanced $\text{NO}_2 + \text{OH}$ reaction, a termolecular reaction with negative dependence on temperature) compensated by reduced production of organic nitrates (through reduced emissions of VOCs). For January, model NO_2 columns are reduced by up to 8 % in some areas (Fig. S9b).

The daytime biases in air temperature exceed 5°C in parts of East China (Fig. S1). Therefore another sensitivity simulation as an extreme case decreases the daytime temperature by 5°C with an enhancement by 1°C at night (Case 3 in Table 1). It reduces model NO_2 columns by 4–10 % in many areas of East China for both months (Fig. 3). Over parts of the southwest, model NO_2 columns are enhanced by up to 16 % in July. Reduced near-surface air temperature in the daytime weakens mixing in the PBL and thus vertical prop-

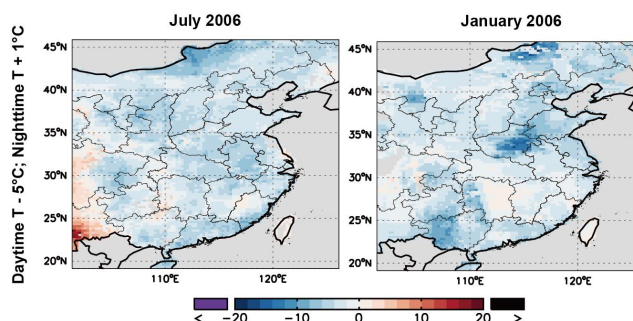


Fig. 3. Spatial distribution of percentage differences between modeled NO_2 columns with and without adjustments in air temperature: the daytime temperature is decreased by 5°C with an increase of 1°C at night for the lowest 10 model layers. See Fig. S9 for more results of sensitivity tests on temperature.

agation of temperature adjustment. Therefore another model experiment constrains the temperature adjustment to the lowest four model layers (i.e., about 0–500 m above the ground) (Case 4 in Table 1). It tends to slightly increase the NO_2 columns relative to when the temperature is adjusted for the lowest 10 layers (Fig. S9e and f versus Fig. 3).

The nighttime temperature errors are not important for simulation of NO_2 columns in the afternoon. This is suggested by an additional simulation increasing the nighttime temperature by 5°C with no changes in the daytime (Case 5 in Table 1). Specifically, the sensitivity test results in insignificant changes in model NO_2 columns in both months: within 2 % for July and within 4 % in most areas for January (not shown).

4.2 Water vapor content

Water vapor content in the troposphere affects the yield of hydroxyl radical (OH) from ozone photolysis and consequently the loss rate of NO_x via OH oxidation. It also affects the hygroscopic growth of hydrophilic aerosols and resulting scattering efficiency for solar radiation. Based on analysis of the GEOS-5 water vapor path in the Supplement, two test simulations are conducted to quantify the sensitivity of model NO_2 columns to errors in water vapor content in GEOS-5. In particular, the water vapor content is scaled up and down, respectively, by a factor of 130 % in all tropospheric layers (Cases 6–7 in Table 1). RH is affected consequently. Increasing the water vapor content results in 4–10 % reductions in NO_2 columns across East China in July with a smaller impact for January (Fig. 4a, b). Decreasing the water vapor content has opposite impacts on model NO_2 columns for both months (Fig. 4c, d).

4.3 Cloud optical depth

Model errors in COD affect the calculation of photolysis for a variety of gaseous tracers (Liu et al., 2009). The COD in

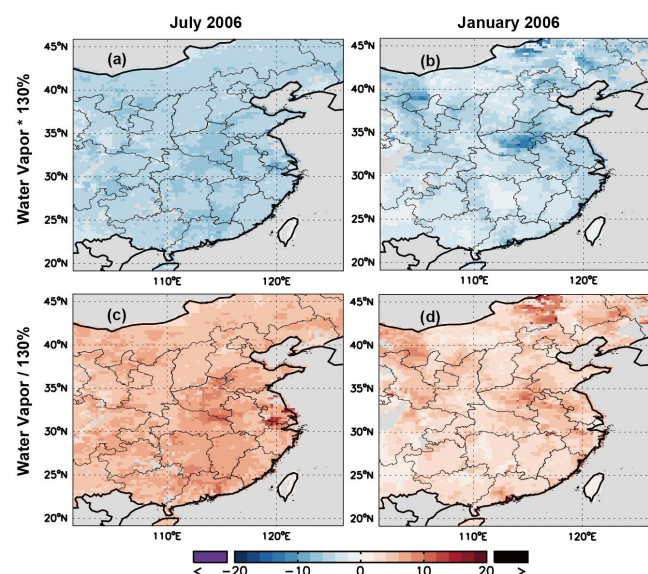


Fig. 4. Spatial distribution of percentage differences between modeled NO_2 columns with and without adjustments in tropospheric water vapor content. (a, b) The water vapor content is scaled up by 130 % in (a, b) and scaled down by 130 % in (c, d).

GEOS-5 is lower than the ISCCP values by 50 % or more in many areas of East China for both January and July (Fig. S7). Here four sensitivity simulations are performed to evaluate the effect of COD on model photolysis and resulting NO_2 columns, by multiplying the COD by a factor of 0 %, 50 %, 150 % and 200 %, respectively (Cases 8–11 in Table 1). Doubling the model COD brings it to within 20 % of ISCCP at most of the places where the unadjusted model COD is much lower than ISCCP. The resulting impacts on NO_2 columns are significant especially in the eastern and southern provinces in July (Figs. 5, S10a–h). In particular, doubling the COD in July enhances modeled NO_2 columns by 20 % or more in many places (Fig. 5), by decreasing solar radiation in the lower troposphere allowed for photodissociation of ozone and NO_2 and formation of OH.

At a given COD, the altitude of clouds affects the vertical distribution of radiation and photolytic activities. In lack of measurements of cloud vertical distribution, the effect of potential model errors is evaluated by a sensitivity simulation distributing the COD evenly in all vertical layers within the troposphere (Case 12 in Table 1). For July, most clouds in GEOS-5 are located in the upper troposphere (not shown). Thus the arbitrary change in cloud vertical profile allows more solar radiation to reach the lower troposphere. This results in a significant increase in the tropospheric OH content with a reduction in NO_2 by up to 16 % (Fig. S10i). For January, most clouds are located in the lower troposphere, especially in the south (not shown); thus the arbitrarily assumed distribution of COD results in slight increases of NO_2 over these regions (Fig. S10j).

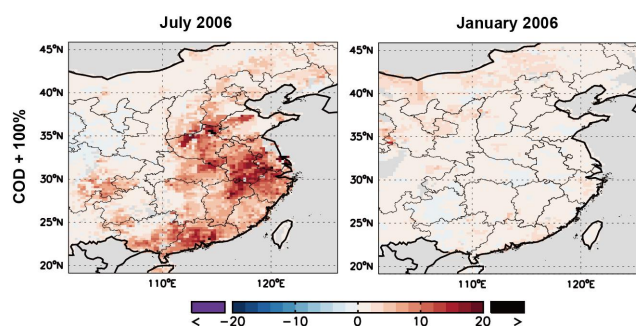


Fig. 5. Spatial distribution of percentage differences between modeled NO_2 columns with and without doubling the COD. See Fig. S10 for more results of sensitivity tests on COD.

4.4 Planetary boundary layer height (PBLH)

Vertical mixing in the PBL of nitrogen and other species affects the non-linear chemical processes in the lower troposphere. It also affects the model–satellite comparison when the altitude-dependent AK (i.e., satellite sensitivity to changes in NO_2 concentrations) is applied to modeled vertical distribution of NO_2 . For instance, enhanced vertical mixing lifts NO_2 to higher altitudes with larger AK and thus enhances the NO_2 column (proxy). In lack of direct observations to evaluate the simulation of PBL mixing for East China, the impact of potential errors is analyzed here by adjusting the PBLH, as surrogate of PBL mixing, in GEOS-Chem (Cases 13–18 in Table 1).

The current GEOS-Chem employs a non-local scheme (Holtslag and Boville, 1993) to determine the extent of vertical mixing in the PBL. Although capable of calculating PBLH, the scheme is set to use the height provided by GEOS-5 as default choice (Lin and McElroy, 2010). The GEOS-5 PBLH is described in the Supplement (Sect. S2). Overall, it may be overestimated in the daytime due to positive biases in surface air temperature enhancing the static instability. At night, it is likely underestimated by a factor of 3, as inferred from the comparison to the observation-based estimate of PBLH for the US by Liu and Liang (2010).

A sensitivity GEOS-Chem simulation allows the non-local scheme to calculate PBLH instead of using the GEOS-5 PBLH (Case 13 in Table 1). For July, this increases the afternoon PBLH over the southeast and northwest with reductions over the southwest (Fig. S11). Consequently, model NO_2 columns are enhanced by 0–4 % near the northern boundary of China, but are reduced by 0–4 % in most areas (Fig. 6a). For January, the afternoon PBLH calculated by GEOS-Chem is higher than the GOES-5 values by 100–200 m over North China (31–41° N, 113–122° E) but is lower over the vast west (Fig. S11). As a result, model NO_2 columns decrease by 2–12 % over most of East China with enhancements by up to 8 % in several provinces (Fig. 6b).

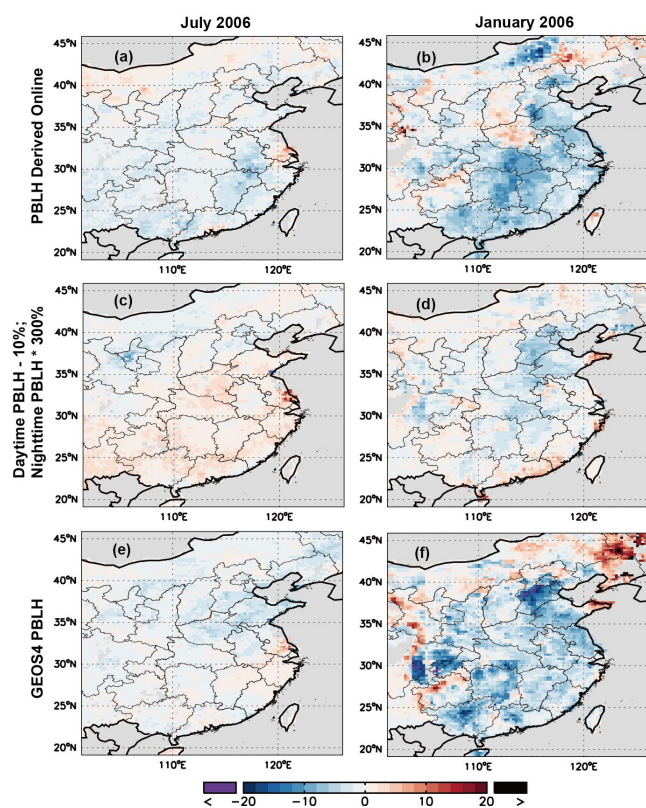


Fig. 6. Spatial distribution of percentage differences between modeled NO_2 columns with and without adjustments in PBLH. (a, b) The PBLH is calculated online by GEOS-Chem instead of being taken directly from GEOS-5. (c, d) The PBLH is decreased by 10 % in the daytime and tripled at night. (e, f) The PBLH is adjusted based on values from the GEOS-4 meteorological fields.

A second sensitivity simulation is conducted by decreasing the PBLH by 10 % in the daytime and tripling the height at night to account for their potential biases (Case 14 in Table 1). For July, this enhances model NO_2 columns by 0–6 % over most regions (Fig. 6c). For January, changes in model NO_2 columns are more inhomogeneous spatially (Fig. 6d). The effects are driven mainly by the enhanced nighttime PBLH, since the adjustment is relatively small for the daytime PBLH. This is confirmed by another simulation tripling the nighttime PBLH with no adjustment in the daytime (Case 15 in Table 1; figures are not shown).

To further test the model sensitivity to PBLH, an additional simulation employs the height data from the GEOS-4 meteorological fields to adjust values in GEOS-5 (Case 16 in Table 1). For a given location and time of day, the ratio of monthly mean GEOS-4 over GEOS-5 PBLH available on the 2.5° long \times 2° lat grid is used to scale the high-resolution GEOS-5 data. The GEOS-4 PBLH is in general higher than GEOS-5 in the nighttime with closer agreement to the observation-based estimate by Liu and Liang (2010). For the mid-day PBLH, the GEOS-4 data are lower than

GEOS-5 over most of East China in January (Fig. S12), resulting in reductions of model NO_2 columns by 0–20 % in many areas (Fig. 6f). They however exceeded the GEOS-5 values in the northeast with a consequent increase in model NO_2 columns. In July, the impacts of PBLH adjustments are within 4 % in most areas for model NO_2 columns (Fig. 6e).

Since NO_2 columns from the base simulation are lower than satellite retrievals by about 20 % in July and 36 % in January averaged over East China, we further test the possibility that the differences originate from errors in modeled PBL mixing. As such, the PBLH is scaled up by 130 % and 200 %, respectively, in two sensitivity simulations (Cases 17–18 in Table 1). For July, increasing the PBLH by 30 % enhances the NO_2 columns by 0–10 % over most regions (Fig. S13a). A 100 % increase in PBLH is used as an extreme case to understand the sensitivity of model NO_2 to PBLH. It results in enhancements of model NO_2 columns by 10–20 % over a large portion of East China (Fig. S13e). The impacts in January are much larger than those for July: model NO_2 columns are enhanced by 10–20 % (20–50 %) in many areas of the east and south when the PBLH is enhanced by 30 % (100 %) (Fig. S13b, f). Considering the impact of PBLH on the nonlinear chemistry alone (i.e., without applying the AK), a 30 % increase in PBLH enhances model NO_2 columns in January by 0–10 % over North China (Case 17 in Table 1) (Fig. S13d).

4.5 Convection and consequent lightning emissions

Convection affects the vertical distributions of NO_x and other species by transporting pollutants between the lower and upper troposphere. It is however highly parameterized and subject to large uncertainties in current models (Tost et al., 2010). As indicators of convection, the cloud amount is underestimated by GEOS-5 while precipitation is reproduced relatively well on the regional mean basis (see Supplement Sects. S1.6 and S1.7). Therefore the magnitude of convection errors in GEOS-5 and consequent impacts on simulations of GEOS-Chem is currently unclear. Lin (2012) conducted a sensitivity analysis assuming a 50 % increase in the convection of NO_2 of anthropogenic origin. They consequently found an increase by 7.5 % in anthropogenic NO_2 columns averaged over East China (when the averaging kernel is applied to modeled vertical distribution of NO_2). Further research is needed to improve the understanding of convection and its representation in the model.

Convection results in lightning flashes and consequent emissions of NO_x . The importance of lightning emissions is affected also by the yield of nitric oxide (NO) from each flash and its vertical distribution, which processes are not well understood (Sauvage et al., 2007). The contribution of a given amount of lightning emissions to model NO_2 columns (when the AK is implemented) is found to be about 50 % larger than that of anthropogenic emissions averaged over East China (Lin et al., 2010b; Lin, 2012). The inverse

modeling by Lin (2012) suggested that GEOS-Chem underestimates lightning emissions in East China by 14 % in July 2006 and by 19 % for the entire year. As a usual practice of top-down emission estimate, lightning emissions are unadjusted when constraining anthropogenic emissions (e.g., Martin et al., 2003; Lin et al., 2010b). Therefore increasing modeled lightning emissions will result in reduced top-down anthropogenic emissions.

5 Sensitivity of GEOS-Chem simulated NO₂ columns to chemical parameters

Originally developed as a global CTM, GEOS-Chem adopts a simplified chemical scheme to reduce the complexness and computational cost for global and regional analyses, as compared to more detailed schemes such as MCM 3.2 (Saunders et al., 2003). It has been suggested that the GEOS-Chem chemical scheme produces relatively consistent results with MCM 3.1 for inorganic gaseous chemistry, taking into account differences in the kinetic data used (JPL versus IUPAC) (Emmerson and Evans, 2009). The differences increase for organic gaseous chemistry (Emmerson and Evans, 2009), as expected for a largely simplified chemical scheme, with potentially important implications for the nitrogen evolution over areas with abundant VOCs. In addition, the implementation of heterogeneous reactions and kinetic data differs between current chemical schemes. In particular, GEOS-Chem mainly adopts the kinetic data from the Jet Propulsion Laboratory (JPL) (Sander et al., 2011), differing from the IUPAC data (Atkinson et al., 2004, 2006) employed in MCM and some other schemes. Therefore the sensitivity analysis here is concentrated on chemical parameters/processes that have been identified to be important for the nitrogen chemistry in general (rather than specific ally to GEOS-Chem) (see Fig. 1 and Table 1). Results here can thus be applied to some extent to other (and maybe more sophisticated) chemical schemes.

5.1 Rate constant for reaction of OH and NO₂

Reaction of OH + NO₂ producing nitric acid (HONO₂, or HNO₃) is the primary sink of NO_x in the troposphere. Recent lab experiments suggested a second pathway producing peroxyxynitrous acid (HOONO) with a branching ratio of 5–15 % under atmospheric conditions (Sander et al., 2011). The newly found pathway has not been accounted for explicitly in the current GEOS-Chem model since HOONO is likely unstable and easily converted back to NO₂. It is excluded from the analysis hereafter.

The current GEOS-Chem adopts the rate constant for the nitric acid branch recommended by the JPL with an uncertainty of 30 % at 298 K (Sander et al., 2011). A recent lab study suggested the rate constant to be about 15 % lower than the JPL value at 298 K without specifying the values at other temperatures (Mollner et al., 2010), in support of some previ-

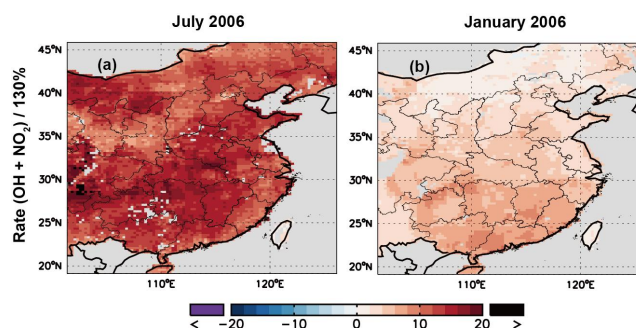


Fig. 7. Spatial distribution of percentage differences between modeled NO₂ columns with and without scaling down the rate constant of OH + NO₂ reaction by a factor of 130 %.

ous studies indicating the current JPL value to be biased high (Okumura and Sander, 2005). Here two sensitivity simulations are performed to evaluate the impact of potential errors in the rate constant on modeled NO₂ columns, by scaling up and down, respectively, the rate constant by a factor of 130 % (Cases 19–20 in Table 1). Decreasing the rate constant enhances model NO₂ columns by 4–20 % across East China in July and by 0–10 % in January (Fig. 7a, b). Increasing the rate constant has an opposite effect of similar magnitude (not shown).

5.2 Yield of HNO₃ from reaction of NO and hydroperoxyl radical (HO₂)

An important pathway of NO₂ formation is reaction of NO and HO₂. Lab experiments by Butkovskaya et al. (2005, 2007, 2009) suggested a small yield of HNO₃ during the reaction resulting in loss of NO_x. The yield depends on temperature, pressure and water vapor content. It is less than 1 % in dry air and increases linearly with increasing concentrations of water vapor (by a factor of 8 from 0 % to 50 % RH at 298 K and 200 Torr; Butkovskaya et al., 2009; Sander et al., 2011). Here, two sensitivity simulations are performed by assuming a constant yield of HNO₃ at 5 % and 1 %, respectively (Cases 21–22 in Table 1). A yield of 5 % reduces model NO₂ columns by 44 % in July and by 12.5 % in January averaged over East China with much larger impacts in many areas (Fig. 8a, b). With a yield of 1 %, model NO₂ columns are reduced by 15 % in July and by 3.4 % in January averaged over East China (Fig. 8c, d). The yield of HNO₃ and its dependence on meteorological conditions is yet to be confirmed by more lab experiments.

5.3 Isoprene + OH reaction, OH-regeneration, isoprene nitrates and PAN

Reaction of isoprene with OH is an important process affecting the budget and partitioning of hydrogen oxide radicals (HO_x). It was assumed traditionally that the reaction resulted in conversion of OH to peroxy radicals (RO₂) and

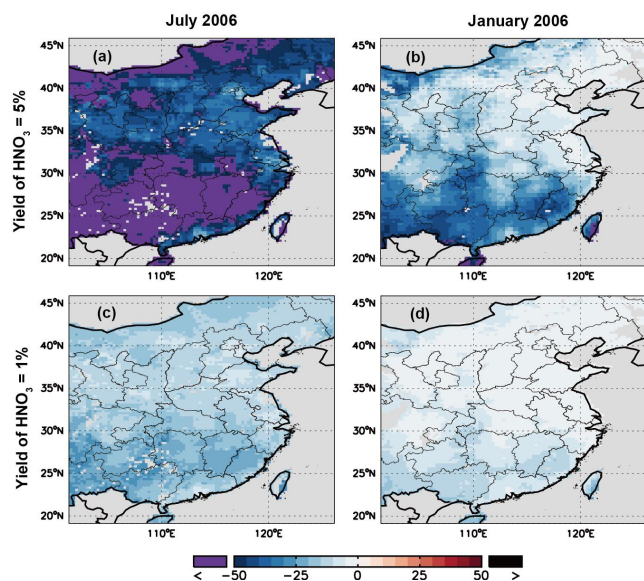


Fig. 8. Spatial distribution of percentage differences between modeled NO_2 columns with and without assuming a yield of HNO_3 at 5% (a, b) or 1% (c, d) from the $\text{HO}_2 + \text{NO}$ reaction.

thus depletion of OH in pristine forested areas with large isoprene sources such as the Amazonian region. More recent research, however, has suggested several pathways of OH regeneration through subsequent reactions of isoprene oxidation products (Butler et al., 2008; Lelieveld et al., 2008; Kubistin et al., 2010). Here two tests are performed to evaluate the effect of isoprene oxidation and OH regeneration on model NO_2 columns. The first test assumes a 100% regeneration of OH from the reaction of isoprene and OH (Case 23 in Table 1) (Kubistin et al., 2010 assumed 130%). This enhances the lower tropospheric (0–2 km) OH content by up to 40% in July over the source regions of isoprene including parts of the southern provinces and the mountain and grassland areas in the north where NO_x concentrations are relatively low (not shown). Consequently, the OH + NO_2 reaction is enhanced and model NO_2 columns decrease by 0–4% over most regions in July with smaller changes of within 2% in January (Fig. 9a, b). Another test is conducted by turning off the reaction of isoprene and OH to prevent the latter from being depleted (Case 24 in Table 1), following Kubistin et al. (2010). As a result, the lower tropospheric (0–2 km) OH content more than doubles in July over parts of the source regions of isoprene with low NO_x (not shown). Over the same regions, model NO_2 columns are increased mostly by 0–20% with a drastic increase by 40–50% in the southwest (Fig. 9c). The increase of NO_2 is attributed to the suppressed formation of isoprene nitrates overcompensating for the effect of enhanced HNO_3 production. The impact is smaller for January 2006 due primarily to lack of isoprene emissions (Fig. 9d).

Production of isoprene nitrates is an important sink of NO_x . It is determined by the yield of isoprene nitrates and

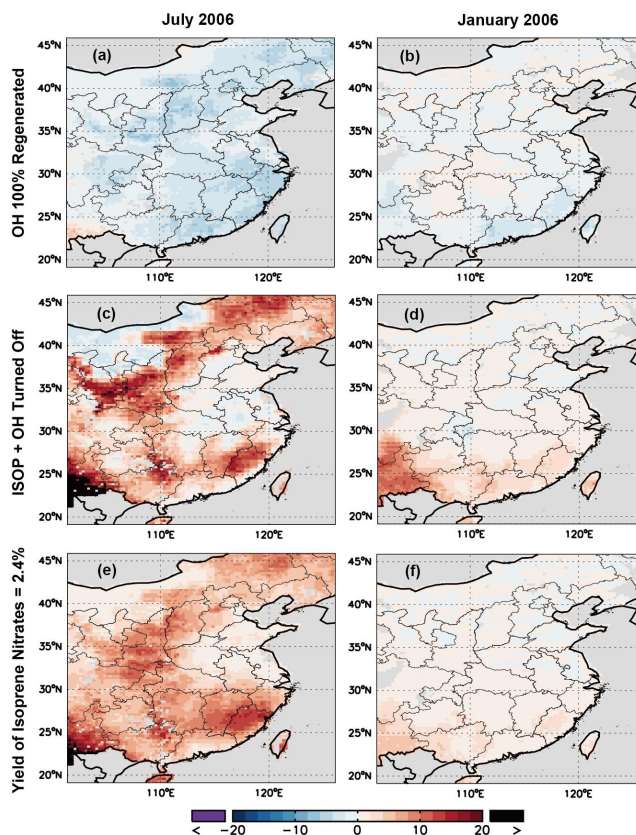


Fig. 9. Spatial distribution of percentage differences between modeled NO_2 columns with and without adjustments in the organic chemistry. (a, b) The OH is assumed to be 100% regenerated from the reaction of isoprene + OH. (c, d) The isoprene + OH reaction is turned off. (e, f) The net yield of isoprene nitrates is assumed to be 2.4% instead of the default 10%.

subsequent partial conversion back to NO_x through photolysis or reactions with OH, i.e., the recycling of NO_x . In addition, certain isoprene nitrates have relatively long atmospheric lifetime and can be transported to downwind areas before being transformed to NO_x (Paulot et al., 2009). These factors affect the abundances of NO_x in source and downwind regions with important consequences on the tropospheric chemistry. For example, previous model studies have suggested large sensitivity of modeled surface ozone concentration to assumptions on production and fate of isoprene nitrates (Fiore et al., 2005; Wu et al., 2007; Lin et al., 2008a, b, c; Ito et al., 2009). The current estimates range from 2.4 to 15% for the net yield of isoprene nitrates (i.e., the amount that does not return to NO_x) (see summary by Paulot et al., 2009). A value of 10%, on the high-end side, is adopted in GEOS-Chem by neglecting transport of the portion of isoprene nitrates decomposed to NO_x . Reducing the net yield to 2.4%, a sensitivity simulation increases the NO_2 columns by up to 25% over the southwest in July and by 0–6% in January (Case 25 in Table 1; Fig. 9e, f).

Production of peroxyacetyl nitrate (PAN) balanced by its thermal decomposition also affects the abundance of NO_2 . Errors in its equilibrium constant are estimated to be about 20 % at 298 K (Sander et al., 2011). A test simulation decreases the constant by 20 %, resulting in slight enhancements of model NO_2 columns by 0–4 % (within 2 % over most regions) in both January and July (Case 26 in Table 1; figures are not shown).

5.4 Heterogeneous reactions involving aerosols

Uptake of HO_2 on aerosols reduces the HO_x content in the troposphere and thus increases the NO_x lifetime. The uptake coefficient depends on aerosol types and meteorological conditions, subject to large uncertainties (Jacob, 2000; Thornton et al., 2008; Kolb et al., 2010; Mao et al., 2010; Macintyre and Evans, 2011; Liu et al., 2012). It can be enhanced by transition metal ions (TMIs) such as copper (Cu) and iron (Fe) contained in aqueous aerosols (Jacob, 2000; Thornton et al., 2008). Thornton et al. (2008) suggested an effective uptake coefficient of 0.04–0.1 on fine-mode pollution aerosols (radius ~ 100 – 200 nm) in the continental boundary layer, based on the mass fraction of Cu in near-surface aerosols observed over the contiguous US. The average value of 0.07 is adopted in the current GEOS-Chem model for sulfate-nitrate-ammonium (SNA) aerosols with no regional dependence. The CTM does not take into account the effect of Fe, as considered to be much lower than that of Cu (Thornton et al., 2008). Meanwhile, the mass fraction of Cu measured in several cities in East China (2.9 – 21.6×10^{-4} in Beijing, Shanghai, Chongqing and Guangzhou) is higher than the average value over the US (1.8×10^{-4}) by a factor of 1.6–12 (He et al., 2001; Thornton et al., 2008; Yang et al., 2011) This is also supported by our preliminary measurement data in Beijing and Shanghai. In Beijing, the fraction of Cu doubled from 2000 to 2005 (He et al., 2001; Yang et al., 2011). Moreover, there is a large fraction of Fe in aerosols in Chinese cities (He et al., 2001; Yang et al., 2011) with potentially important impacts on the uptake of HO_2 , due not just to its sole catalytic effect but also to its potential interactions with Cu enhancing the effects of both TMIs (Mao et al., 2012). Given the amount of TMIs, the uptake coefficient in these Chinese cities is likely to be much larger than currently assumed in the model, as supported by recent field measurements (Taketani et al., 2012). In a sensitivity simulation, the coefficient is increased to 0.2 in the troposphere over China (Case 27 in Table 1), a value consistent with previous estimates based on field measurements in North America and Hawaii (see review by Jacob, 2000). As a result, model NO_2 columns in July are enhanced by 4–14 % over North China with smaller impacts in other areas (Fig. 10a). In January, model NO_2 columns increase by up to 50 % in many areas (Fig. 10b). Another sensitivity simulation changes the uptake coefficient to 0.2 on SNA aerosols in the PBL over China (Case 28 in Table 1). It

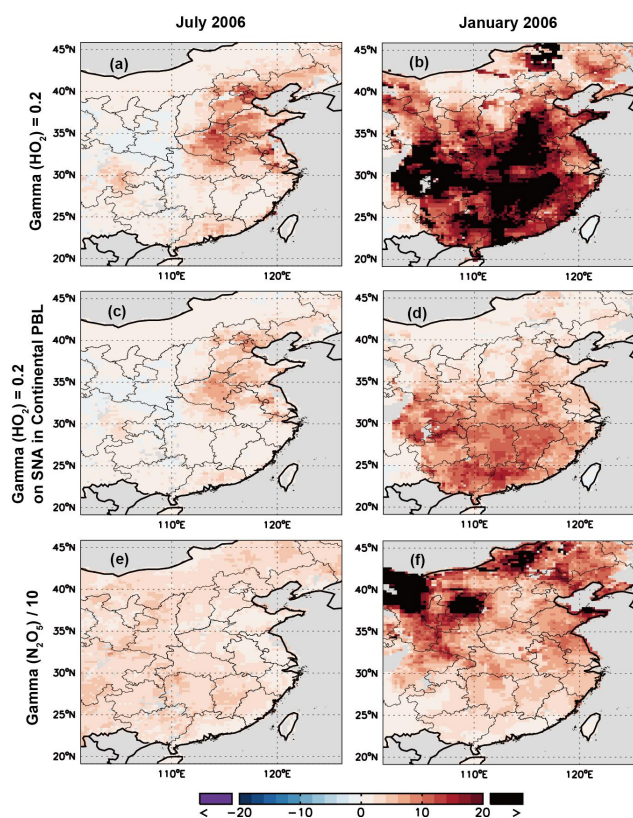


Fig. 10. Spatial distribution of percentage differences between modeled NO_2 columns with and without adjustments in the heterogeneous chemistry. (a, b) The uptake rate of HO_2 on aerosols is assumed to be 0.2. (c, d) The uptake rate of HO_2 on sulfate-nitrate-ammonium aerosols is assumed to be 0.2 in the continental boundary layer. (e, f) The uptake rate of N_2O_5 on aerosols is scaled down by a factor of 10.

thus increases the NO_2 columns by 2–10 % over North China in July and by 2–16 % over the south in January (Fig. 10c, d).

Heterogeneous reaction of nitrogen pentoxide (N_2O_5) on aerosol surfaces is an important sink of NO_x , especially at night and in winter with relatively weak photochemistry. The uptake coefficient of N_2O_5 depends on aerosol types and meteorological conditions, as parameterized in the current GEOS-Chem (Evans and Jacob, 2005). More recent lab experiments suggested the coefficient to be lower than the Evans and Jacob (2005) estimate by a factor of up to 10 with dependence on meteorological conditions that is still not clear (Bertram et al., 2009; Brown et al., 2009). A sensitivity simulation reduces the uptake coefficient by an order of magnitude (Case 29 in Table 1). It consequently increases model NO_2 columns by 0–6 % over most regions in July and by more than 50 % over part of the northwest in January (Fig. 10e, f). The results are consistent with Lin and McElroy (2011).

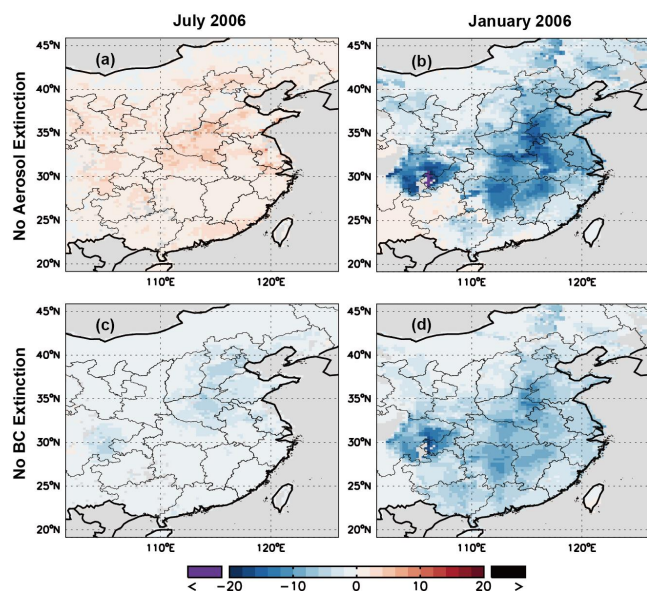


Fig. 11. Spatial distribution of percentage differences between modeled NO_2 columns with and without eliminating the scattering and absorption of radiation by all aerosols (a, b) or BC (c, d).

5.5 Aerosol optical properties

The tropospheric photochemistry is affected by the amount of solar radiation scattered or absorbed by aerosols. Figures S14 and S15 compare modeled AOD with MODIS/Aqua measurements. In July, GEOS-Chem underestimates the MODIS AOD by 10–50 % in many areas of East China (Fig. S14). This is in part because the formation of secondary organic aerosols is not accounted for with the current model setup. For January, however, the CTM overestimates MODIS AOD by more than 100 % in many places (Fig. S15). Further research is required to fully understand the causes of these differences.

Two test simulations are performed here to quantify the impacts of aerosol scattering and absorption on model NO_2 columns. The first test turns off both scattering and absorption of aerosols in calculating the photochemistry (Case 30 in Table 1). It thus increases model NO_2 columns in July by 0–6 % over most regions but has a negative impact of 10–20 % in January for a large portion of East China (Fig. 11a, b). Another test turns off the effect of black carbon alone resulting in reductions of NO_2 by 0–6 % in July and by up to 20 % in January (Case 31 in Table 1; Fig. 11c, d). The differences (magnitude and sign) are evident between the two tests and between the two months. It is because most aerosols and NO_x are collocated in the PBL, in which situation scattering by aerosols alone tends to increase the actinic flux for photodissociation of NO_2 while absorption by aerosols decreases the actinic flux. In July, the amount of black carbon (emitted mostly from the residential sector) is small relative to scattering aerosols, resulting in a dominant effect by scattering.

In January, the concentration of black carbon increases; thus the aerosol scattering enhances the effect of absorption by providing more diffuse radiation, resulting in enhanced reduction of the actinic flux.

5.6 Emissions

Emissions of CO and (to a lesser extent) SO_2 affect the OH content with consequences on the reaction of OH and NO_2 and other related photochemical processes. For example, lower CO and SO_2 emissions result in higher OH and consequently lower lifetime and concentration of NO_2 . Large uncertainties exist in current emission estimates based on both bottom-up and top-down approaches (Fortems-Cheiney et al., 2011; Lu et al., 2011). That the simulated NO_2 is lower than satellite measurements (Lin, 2012) may be caused partially by possible underestimates of CO and SO_2 emissions in the INTEX-B inventory. Therefore a test simulation is performed here by increasing CO and SO_2 emissions by 50 % (Case 32 in Table 1); such amount of increase accounts for uncertainties in the INTEX-B inventory (Zhang et al., 2009b). As a result, the model NO_2 columns are enhanced by up to 6 % over North China in July and by up to 10 % over the south in January (Fig. S16a, b).

Emissions of VOCs affect OH and other radicals with consequences on the formation of HNO_3 and organic nitrates. Recent ground- and space-based measurements have suggested anthropogenic emissions of aromatics to be underestimated by a factor of 4–10 over East China in the INTEX-B inventory employed here (Liu et al., 2010, 2011). Meanwhile, the current model setup does not include the simulation of aromatics, preventing a direct evaluation of their impacts on model NO_2 columns. Analysis on propene and aromatics, however, suggests similarity in reactivity and oxidation products with respect to OH, although differences exist in the formation of alkyl nitrates and PAN. This points to a possibility of using propene as a proxy of aromatics in the model for purposes of sensitivity evaluation. Based on the reactivity and emission strength (provided from INTEX-B), it is estimated that assuming an extra source (50 %) of propene can roughly represent the effect of aromatics on the nitrogen chemistry in accordance with the emission inventory. Therefore two tests are performed here to indirectly evaluate the impact of aromatics on model NO_2 columns, by increasing emissions of propene by 50 % and 300 % (i.e., assuming emissions of aromatics to be six times as much as INTEX-B), respectively (Cases 33–34 in Table 1). The 50 % increase in propene emissions results in small changes (i.e., within 2 %) in model NO_2 columns for both months (Fig. S16c, d). Increasing emissions of propene by 300 % enhances the NO_2 columns by 0–4 % over most regions in July with a negative effect of 0–20 % in most areas in January (Fig. 12). The different signs and magnitudes of NO_2 changes in the two months are attributed mainly to enhanced formation of PAN

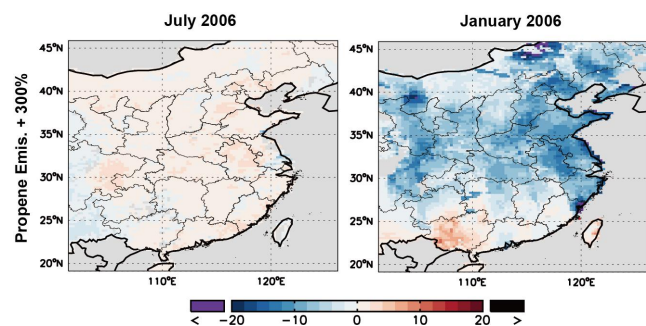


Fig. 12. Spatial distribution of percentage differences between modeled NO_2 columns with and without increasing emissions of propene by 300 %. See Fig. S16 for more results of sensitivity tests on non- NO_x emissions.

compensated by the effect of reduced production of HNO_3 through the $\text{NO}_2 + \text{OH}$ reaction.

A further simulation increases emissions of CO , SO_2 and VOC (including VOC from vegetation) together by 50 %, following Lin et al. (2010b) (Case 35 in Table 1). As a result, model NO_2 columns in July increase by up to 6 % over North China but decrease by up to 20 % over the southwest (Fig. S16g). The reduction in the southwest is attributed mainly to the increased formation of organic nitrates. In January, changes in model NO_2 columns are within 4 % over most regions (Fig. S16h).

Emissions of NO_x assumed in GEOS-Chem may also affect the lifetime of NO_x and its partitioning into NO and NO_2 through the nonlinear chemical process. For East China, anthropogenic sources account for about 77 % of total NO_x emissions in July 2006 and 92 % annually. Biomass burning sources are negligible, and soil and lightning sources are largely collocated with anthropogenic sources (Lin, 2012). In polluted areas, the CTM significantly underestimates NO_2 columns as compared to satellite measurements (Fig. 2a, b), pointing to potentially large negative biases in the a priori emissions (Lin, 2012). In cleaner areas with larger contributions from natural sources, model NO_2 columns are more comparable to satellite data (Fig. 2a, b) suggesting smaller biases in the a priori emissions. Overall, the effect of NO_x emission biases on the nonlinearity of nitrogen chemistry is within 10 % for both January and July on the regional mean basis (Martin et al., 2006; Lin and McElroy, 2011; Lin, 2012).

5.7 Other mechanisms and issues

Several new mechanisms have been proposed in recent years that may also affect the abundances of NO_x in the troposphere, including a reaction of NO_2 with water vapor to produce nitrous acid (HONO) (Li et al., 2008), a potential source of HONO from soil nitrates (Su et al., 2011), and much larger dry deposition of VOC over deciduous ecosystems than pre-

viously thought (Karl et al., 2010). A detailed discussion is presented in the Supplement (Sect. S3). Given the large uncertainties, these mechanisms are not included in most CTMs and are not evaluated quantitatively here.

Valin et al. (2011) suggested a potentially significant nonlinear effect of model horizontal resolution on simulations of NO_2 due to the interaction between NO_x and HO_x , based on chemical mechanism arguments and 7 days of WRF-Chem simulations (1–7 July 2006). The effect is highly location and time dependent as affected by the varying meteorological and chemical conditions. It is expected to be smaller in winter (with lengthened lifetime and enhanced horizontal homogeneity of NO_x loosening the requirement on model resolution) than in summer. Vertical resolution may also be important for nitrogen simulations considering the large vertical gradient of NO_x and other related species (Lin and McElroy, 2010). Further research is needed to fully quantify the resolution-induced model errors.

6 Modifying model NO_2 columns accounting for errors in meteorology and chemistry

Model NO_2 columns can be modified on the first order by linearizing the impacts of errors in meteorological and chemical parameters:

$$\begin{aligned} \ln(\Omega) &= f(P_i), \quad i = 1, 2, 3, \dots \\ &\approx \ln \Omega_0 + \sum (\partial \ln \Omega / \partial P_i \cdot \Delta P_i) \\ \Rightarrow \Omega &= \Omega_0 \cdot e^{\sum (\partial \ln \Omega / \partial P_i \cdot \Delta P_i)} \end{aligned} \quad (1)$$

where Ω represents the post-modification NO_2 columns, Ω_0 represents modeled NO_2 columns prior to the modifications, P_i represents a particular meteorological or chemical parameter, and $f(P_i)$ represents the CTM. $\partial \ln \Omega / \partial P_i$ is derived from the sensitivity simulations, and ΔP_i is the quantified errors of the given parameter based on current knowledge. The modifications are done for grid boxes (at 0.25° long \times 0.25° lat) with respect to the 284 ground meteorological stations, assuming that the impacts are local for NO_2 columns. To partially account for the effect of horizontal transport, the NO_2 columns are smoothed with values from the surrounding eight grid boxes (i.e., 3 grid boxes by 3 grid boxes smoothing) prior to the modifications.

Parameters considered for post-model modification include air temperature, water vapor content, COD, uptake coefficients on aerosols for HO_2 and N_2O_5 , rate constant for reaction of OH and NO_2 , OH regeneration from the isoprene chemistry, net yield of isoprene nitrates, aromatics (as represented by the 300 % increase in propene emissions), and scattering and absorption of radiation by aerosols (see Table 2). Parameters not accounted for in the modification are discussed in the Supplement (Sect. S4). As detailed in Table 2, the observed meteorological parameters are taken from the ISH and ISCCP datasets for parameter error calculations. The modeled effect of aerosol scattering

Table 2. Parameters considered in post-model modification for NO₂ columns at the 284 meteorological stations in East China.

Parameter	Modifications	Case in Table 1 ¹	Impacts on NO ₂ columns ²	Notes and references
(a) Air temperature	Based on ISH values	3	Insignificant	Modification is assumed for the lowest 10 layers
(b) Tropospheric water vapor content	Based on ISCCP values	7	Small in July and insignificant in January	
(c) Cloud optical depth	Based on ISCCP values	11	Very large in July and insignificant in January	
(d) Rate constant of OH + NO ₂ reaction	Lowered by 15 %	19	Large in July and small in January	Mollner et al. (2010); Sander et al. (2011)
(e) OH regeneration from isoprene chemistry	Yield of 100 % from isoprene + OH reaction assumed	23	Small in July and insignificant in January	Butler et al. (2008); Lelieveld et al. (2008); Kubistin et al. (2010)
(f) Net yield of isoprene nitrates	6 % instead of 10 %	25	insignificant	See review by Paulot et al. (2009)
(g) Uptake rate of HO ₂ on aerosols	0.2 instead of the default setup; biases in model AOD with respect to MODIS accounted for	27	Very large	Thornton et al. (2008); Jacob (2000); He et al. (2001); Yang et al. (2011)
(h) Uptake rate of N ₂ O ₅ on aerosols	10 % of the default setup; biases in model AOD with respect to MODIS accounted for	29	Insignificant in July and large in January	Bertram et al. (2009); Brown et al. (2009)
(i) Aerosol scattering and absorption	Scaled based on MODIS AOD in comparison with model AOD	30	Insignificant	
(j) Emissions of propene	Increased by 300 %	34	Insignificant in July and large in January	To represent effects of aromatics based on top-down constraint (Liu et al., 2010, 2011)

¹ Results from sensitivity simulations described in Table 1 are used as the basis of respective post-model modifications here; i.e., they provide $\partial \ln \Omega / \partial P_i$ in Eq. (1) for individual parameters.

² Impacts with the slopes in Figs. 13–14 deviating from unity by more than 10 %, 5–10 %, 2–5 %, and within 2 % are indicated here as very large, large, small, and insignificant, respectively. Note that these indications are for the overall impact in East China; impacts may be larger or smaller at individual stations.

and absorption is adjusted based on the comparison between model and MODIS AOD. The rate constant for OH + NO₂ reaction is taken to be 15 % lower than adopted in the CTM (Mollner et al., 2010; Sander et al., 2011). The net yield of isoprene nitrates is estimated at 6 % instead of 10 % (Paulot et al., 2009), neglecting for simplicity the horizontal transport of isoprene nitrates affecting the spatial distribution of NO_x. The uptake coefficient of N₂O₅ on aerosols is taken to be 10 % of the value adopted in GEOS-Chem (Bertram et al., 2009; Brown et al., 2009) as a highly simplified modification. A more appropriate value of 0.2 is assumed for the uptake coefficient of HO₂ to account for the large amount of TMIs

in China (He et al., 2001; Thornton et al., 2008; Yang et al., 2011), as a rough estimate. In analyzing the uptake of HO₂ and N₂O₅, the surface areas of aerosols are scaled by the ratio of MODIS AOD to model values. Note that the range of parameter errors adopted here contains uncertainties to some extent, and nonlinearity in the impact of parameter errors on model NO₂ columns is not fully accounted for. Our simplified modifications serve only to roughly infer the impacts of potential errors in model meteorology and chemistry; they cannot be interpreted literally as true apportionment of model errors.

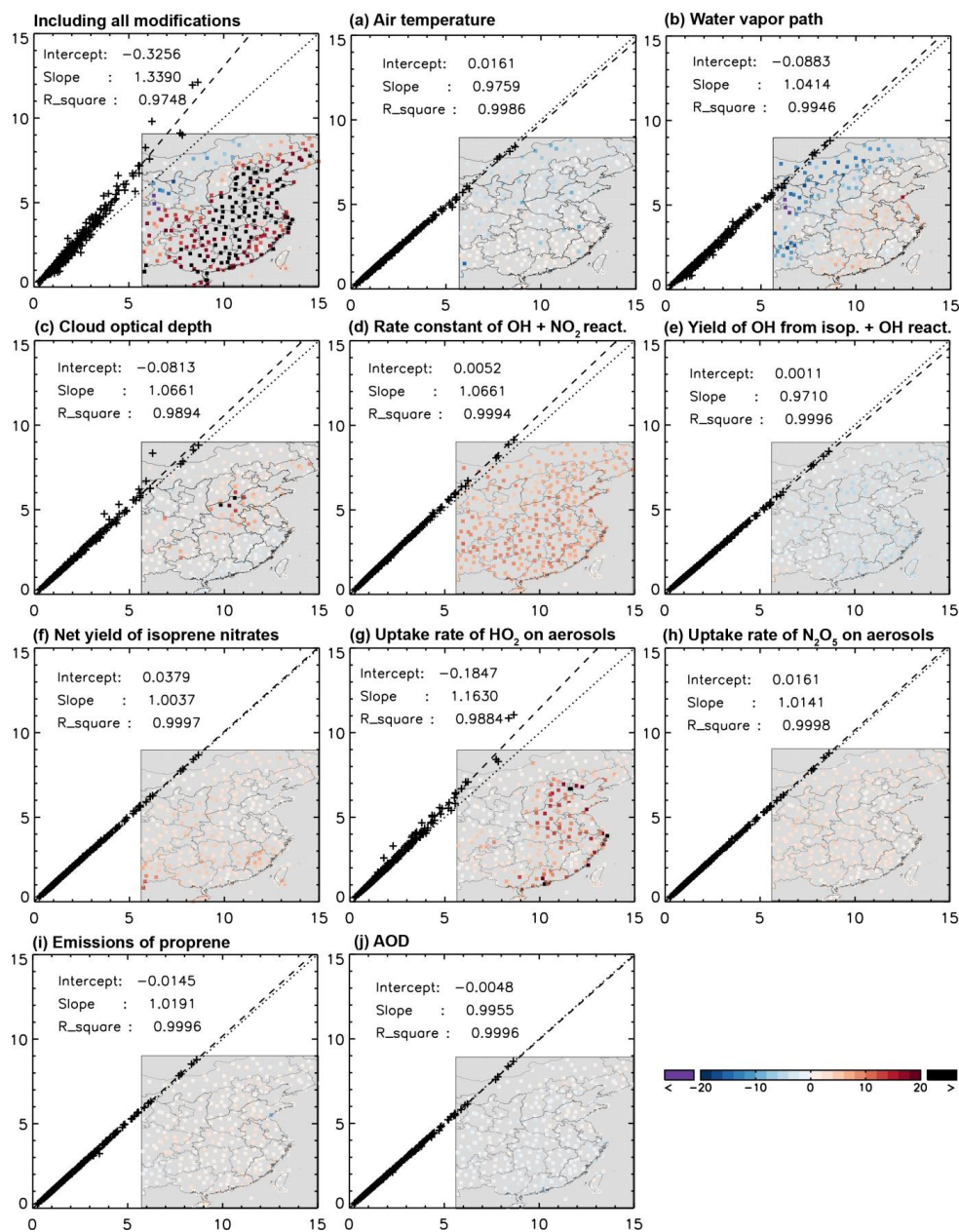


Fig. 13. Scatter plot for model NO_2 columns (10^{15} molec. cm^{-2}) in July 2006 without (x-axis) and with (y-axis) post-model modifications accounting for errors in meteorological and chemical parameters. Cases (a–j) are described in order in Table 2. Embedded in each panel are the respective statistics from the RMA regression and the spatial distribution of their percentage differences.

Table 2 and Figs. 13–14 compare the NO_2 columns with and without post-model modifications. Figures 13–14 also present results of the RMA regression for NO_2 columns pre- and post-modifications. Modification accounting for the uptake coefficient of HO_2 on aerosols has the largest impact on NO_2 columns across East China, resulting in a slope of about 1.16 in July and 1.10 in January (Figs. 13g, 14g). Modification for COD also has a large impact in July with a slope of about 1.07 (Fig. 13c). Modifications for the rate constant

of $\text{OH} + \text{NO}_2$ reaction and the approximate representation of aromatics using propene have important consequences in July and January, respectively (Figs. 13d, 14i).

Taking into account all modifications, the resulting NO_2 columns are highly correlated with the values prior to the modifications (Figs. 13a, 14a). They however are larger than model values in most places with a slope of about 1.34 in July and 1.07 for January under the RMA regression (Figs. 13a, 14a). Averaged over the stations, all modifications combined

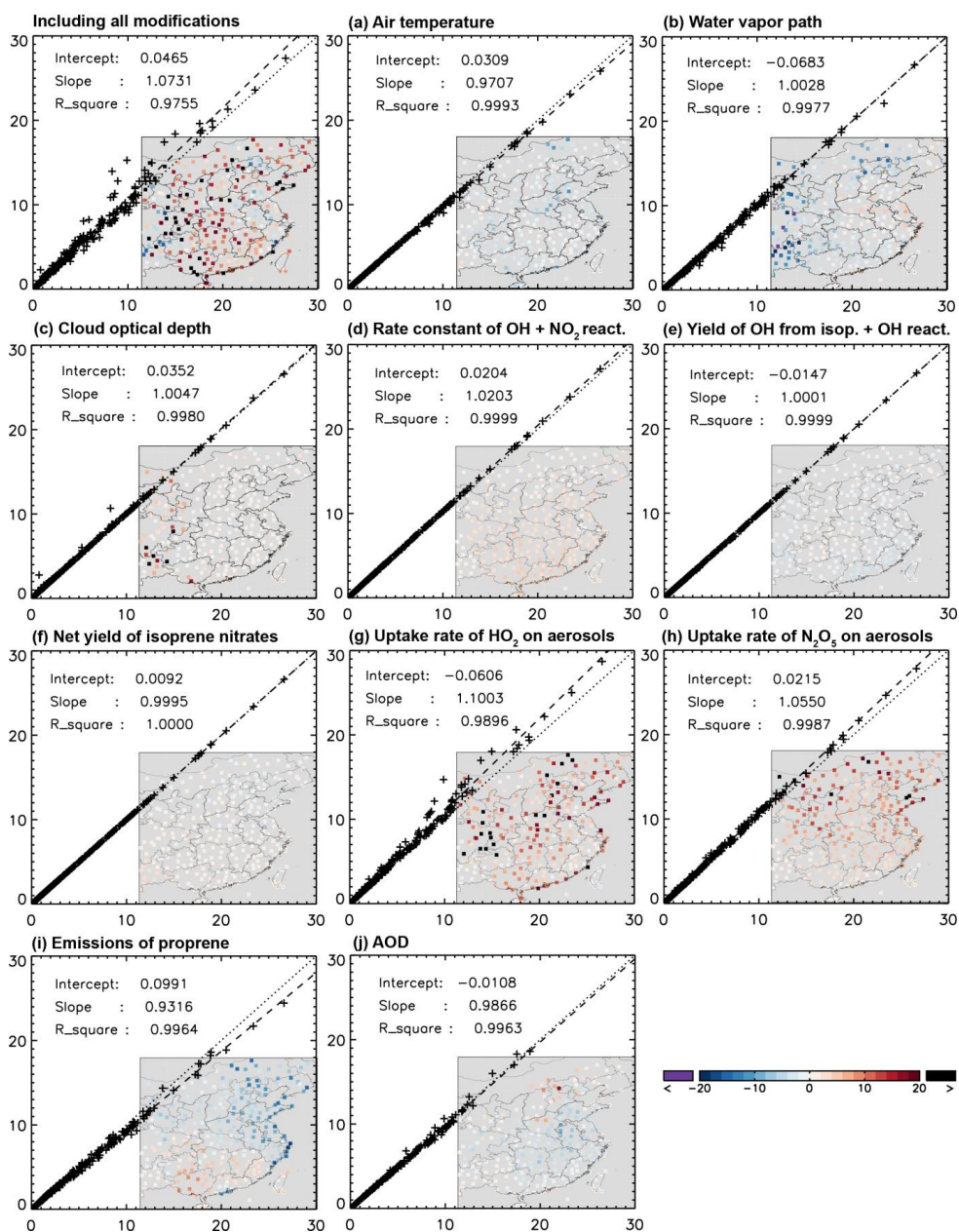


Fig. 14. Similar to Fig. 13 but for January 2006.

increase the NO₂ columns by 18 % in July and by 8 % in January. This suggests significant systematic biases in GEOS-Chem with important consequences on the inverse modeling of NO_x emissions and other related applications. That model errors are likely larger in summer than in winter is in broad consistency with the findings of Huijnen et al. (2010) for Europe. Based on results here and previous analyses on random errors of GEOS-Chem (e.g., Martin et al., 2003; Lin and McElroy, 2011), a conservative estimate suggests the current model to contain a negative systematic bias of 10–20 % (season-dependent) plus a random error of 30 % for NO₂ col-

umn simulations over East China. The random error accounts for regional dependence of model biases, uncertainties in the range of meteorological/chemical parameters for post-model modification and nonlinearity issues during the process, and error sources that are not explicitly taken into account here (e.g., emissions affecting the nonlinearity of nitrogen chemistry, etc.).

Van Noije et al. (2006) compared NO₂ columns for 2000 simulated by nine global models differing in spatial resolution, meteorological inputs, soil/lightning emissions, uptake of N₂O₅ on aerosols and other gaseous and heterogeneous

chemical mechanisms. They found results for both July and January over eastern China (110–123° E, 30–40° N) from three models to be different by up to 50 % from six other models providing more consistent simulations (including GEOS-Chem). Van Noije et al. (2006) also found large inter-model spread in Europe, as confirmed by Huijnen et al. (2010) evaluating eight regional models and two global models. The inter-model differences in simulated NO₂ columns are likely because errors in meteorological/chemical parameters are inconsistent in sign and/or magnitude across the models. For example, parameters and processes may be overestimated by some models but neglected/underestimated by other models.

The modified columns are still lower than satellite retrievals with a slope of about 0.66 in July and 0.53 in January (Fig. 2c, d). The negative biases are driven mainly by those in polluted areas with retrieved NO₂ columns exceeding 6×10^{15} molec. cm⁻² in July and 12×10^{15} molec. cm⁻² in January. For cleaner areas, the slope increases to about 1.0 in July and 0.88 in January.

7 Conclusions

Potential errors are evaluated in this study for the nested GEOS-Chem simulations of tropospheric NO₂ columns over East China for satellite-based emission inversion. Driven by the GEOS-5 meteorological fields and the INTEX-B anthropogenic emissions, the model underestimates NO₂ columns retrieved from OMI (DOMINO-2) by 20 % in July 2006, by 36 % in January 2006, and by a factor of 3–5 in extremely polluted areas (Lin, 2012). In lack of sufficient in-situ measurements of nitrogen for direct model evaluation, a systematic analysis is conducted for meteorological and chemical parameters affecting the simulation of NO_x. The analysis is focused in January and July 2006 to evaluate the seasonal dependence of model sensitivity to meteorology and chemistry. Many of the model issues found for GEOS-Chem are also relevant to other CTMs.

Errors in the GEOS-5 meteorological fields are evaluated with observations from the ground network (NCDC ISH) and from space (ISCCP). GEOS-5 significantly underestimates cloud fraction and cloud optical depth over East China as compared to measurements from ISCCP. It also contains errors of regional and seasonal dependence in air temperature, relative humidity, water vapor content, wind speed and precipitation. Sensitivity simulations suggest that the impacts of these errors on modeled NO₂ columns are normally below 20 % across East China.

Model NO₂ columns are also sensitive to PBLH as surrogate of PBL mixing (especially when the averaging kernel from the satellite product is applied to simulated vertical distribution of NO₂). However, an unrealistically 100 % increase in PBLH still cannot eliminate the negative model biases in extremely polluted areas relative to satellite data.

A variety of chemical parameters is also evaluated with the CTM based on current understanding of their uncertainties. Factors considered include the rate constant for reaction of OH + NO₂, yield of HNO₃ from reaction of NO + HO₂, OH regeneration from the isoprene chemistry, yield and fate of isoprene nitrates, equilibrium constant for formation and thermal decomposition of PAN, uptake coefficients on aerosols for HO₂ and N₂O₅, chemistry of aromatics, emissions of CO, VOC and SO₂, and scattering and absorption of solar radiation by aerosols. Perturbations on these factors affect simulated NO₂ columns by various magnitudes strongly depending on regions and seasons.

In order to understand the overall uncertainty of GEOS-Chem, modeled NO₂ columns are modified at the 284 ground meteorological stations in East China by accounting for errors in various meteorological and chemical parameters. The modifications together increase the NO₂ columns by 18 % in July and by 8 % in January averaged across the stations, likely indicating systematic model errors. They result in closer agreement with satellite retrievals, but cannot eliminate the negative biases in extremely polluted places. Individually, assuming the uptake coefficient of HO₂ on aerosols to be 0.2 (to account for the large amount of transition metal ions) has the largest impact on NO₂ columns, followed by corrections on COD, rate constant of OH + NO₂ reaction, uptake coefficient of N₂O₅ on aerosols, and inclusion of aromatics.

Based on results here and previous works (e.g., Martin et al., 2003; Lin and McElroy, 2011), a negative systematic bias of 10–20 % (season-dependent) plus a random error of 30 % seems appropriate for GEOS-Chem simulations over East China.

As a concluding remark, we further address the large differences between modeled and retrieved tropospheric NO₂ columns in extremely polluted areas. Model errors appear not to be the primary cause based on the present analysis. Satellite retrievals are sensitive to assumptions on stratospheric NO₂, aerosols, clouds, surface reflectance, terrain height, and a priori vertical profile of NO₂. Most aerosols of anthropogenic origin are collocated with NO₂ in the PBL, affecting the amount of solar radiation absorbed by NO₂. The presence of aerosols is not accounted for explicitly in current satellite NO₂ products; their scattering effect is treated implicitly as arbitrarily enhanced cloud fraction. The sensitivity of NO₂ columns on aerosol scattering and absorption is found in this study to be within 20 % across East China, a value much smaller than the magnitude of model underestimates in extremely polluted areas. The presence of aerosols may also affect the retrieval of surface reflectance with consequences on subsequent cloud and NO₂ retrievals. This factor cannot likely account for the large model underestimates in extremely polluted areas. In addition, errors (in percentage) in satellite retrievals caused by non-aerosol factors are not expected to be highly correlated to the amount of NO₂. Therefore retrieval errors seem unlikely to be the main source

of model-retrieval differences in extremely polluted areas. It appears that the differences are derived largely from the underestimate of NO_x emissions in the INTEX-B inventory used to drive the model simulations (e.g., dilution of point sources when converted to gridded data, underestimate of industrial sources, etc.).

Supplementary material related to this article is available online at: <http://www.atmos-chem-phys.net/12/12255/2012/acp-12-12255-2012-supplement.pdf>.

Acknowledgements. This research is supported by the National Natural Science Foundation of China, grant 41005078 and 41175127. The work of G. Zhuang is supported by the great international collaboration project of MOST, China (2010DFA92230), National Natural Science Foundation of China (Grant No. 41128005, fund for collaboration with oversea scholars). We acknowledge the free use of tropospheric NO₂ column data from www.temis.nl, MODIS AOD data from NASA, and meteorological data from NOAA NCDC and the ISCCP project. We thank Randall V. Martin and Mathew Evans for useful comments.

Edited by: L. Ganzeveld

References

- Atkinson, R., Baulch, D. L., Cox, R. A., Crowley, J. N., Hampson, R. F., Hynes, R. G., Jenkin, M. E., Rossi, M. J., and Troe, J.: Evaluated kinetic and photochemical data for atmospheric chemistry: Volume I – gas phase reactions of O_x, HO_x, NO_x and SO_x species, *Atmos. Chem. Phys.*, 4, 1461–1738, doi:10.5194/acp-4-1461-2004, 2004.
- Atkinson, R., Baulch, D. L., Cox, R. A., Crowley, J. N., Hampson, R. F., Hynes, R. G., Jenkin, M. E., Rossi, M. J., Troe, J., and IUPAC Subcommittee: Evaluated kinetic and photochemical data for atmospheric chemistry: Volume II – gas phase reactions of organic species, *Atmos. Chem. Phys.*, 6, 3625–4055, doi:10.5194/acp-6-3625-2006, 2006.
- Bertram, T. H., Thornton, J. A., Riedel, T. P., Middlebrook, A. M., Bahreini, R., Bates, T. S., Quinn, P. K., and Coffman, D. J.: Direct observations of N₂O₅ reactivity on ambient aerosol particles, *Geophys. Res. Lett.*, 36, L19803, doi:10.1029/2009gl040248, 2009.
- Boersma, K. F., Jacob, D. J., Bucsela, E. J., Perring, A. E., Dirksen, R., van der A, R. J., Yantosca, R. M., Park, R. J., Wenig, M. O., Bertram, T. H., and Cohen, R. C.: Validation of OMI tropospheric NO₂ observations during INTEX-B and application to constrain NO_x emissions over the eastern United States and Mexico, *Atmos. Environ.*, 42, 4480–4497, doi:10.1016/j.atmosenv.2008.02.004, 2008.
- Boersma, K. F., Jacob, D. J., Trainic, M., Rudich, Y., DeSmedt, I., Dirksen, R., and Eskes, H. J.: Validation of urban NO₂ concentrations and their diurnal and seasonal variations observed from the SCIAMACHY and OMI sensors using in situ surface measurements in Israeli cities, *Atmos. Chem. Phys.*, 9, 3867–3879, doi:10.5194/acp-9-3867-2009, 2009.
- Boersma, K. F., Eskes, H. J., Dirksen, R. J., van der A, R. J., Veefkind, J. P., Stammes, P., Huijnen, V., Kleipool, Q. L., Sneep, M., Claas, J., Leitão, J., Richter, A., Zhou, Y., and Brunner, D.: An improved tropospheric NO₂ column retrieval algorithm for the Ozone Monitoring Instrument, *Atmos. Meas. Tech.*, 4, 1905–1928, doi:10.5194/amt-4-1905-2011, 2011.
- Brinkma, E. J., Pinardi, G., Volten, H., Braak, R., Richter, A., Schonhardt, A., van Roozendaal, M., Fayt, C., Hermans, C., Dirksen, R. J., Vlemmix, T., Berkhout, A. J. C., Swart, D. P. J., Oetjen, H., Wittrock, F., Wagner, T., Ibrahim, O. W., de Leeuw, G., Moerman, M., Curier, R. L., Celarier, E. A., Cede, A., Knap, W. H., Veefkind, J. P., Eskes, H. J., Allaart, M., Rothe, R., PETERS, A. J. M., and Levelt, P. F.: The 2005 and 2006 DANDELIONS NO₂ and aerosol intercomparison campaigns, *J. Geophys. Res.-Atmos.*, 113, D16S46, doi:10.1029/2007jd008808, 2008.
- Brown, S. S., Dube, W. P., Fuchs, H., Ryerson, T. B., Wollny, A. G., Brock, C. A., Bahreini, R., Middlebrook, A. M., Neuman, J. A., Atlas, E., Roberts, J. M., Osthoff, H. D., Trainer, M., Fehsenfeld, F. C., and Ravishankara, A. R.: Reactive uptake coefficients for N₂O₅ determined from aircraft measurements during the Second Texas Air Quality Study: Comparison to current model parameterizations, *J. Geophys. Res.-Atmos.*, 114, D00F10, doi:10.1029/2008jd011679, 2009.
- Butkovskaya, N. I., Kukui, A., Pouvesle, N., and Le Bras, G.: Formation of nitric acid in the gas-phase HO₂+NO reaction: Effects of temperature and water vapor, *J. Phys. Chem. A*, 109, 6509–6520, doi:10.1021/jp051534v, 2005.
- Butkovskaya, N., Kukui, A., and Le Bras, G.: HNO₃ forming channel of the HO₂+NO reaction as a function of pressure and temperature in the ranges of 72–600 torr and 223–323 K, *J. Phys. Chem. A*, 111, 9047–9053, doi:10.1021/jp074117m, 2007.
- Butkovskaya, N., Rayez, M.-T., Rayez, J.-C., Kukui, A., and Le Bras, G.: Water Vapor Effect on the HNO₃ Yield in the HO₂ + NO Reaction: Experimental and Theoretical Evidence, *J. Phys. Chem. A*, 113, 11327–11342, doi:10.1021/jp811428p, 2009.
- Butler, T. M., Taraborrelli, D., Brühl, C., Fischer, H., Harder, H., Martinez, M., Williams, J., Lawrence, M. G., and Lelieveld, J.: Improved simulation of isoprene oxidation chemistry with the ECHAM5/MESy chemistry-climate model: lessons from the GABRIEL airborne field campaign, *Atmos. Chem. Phys.*, 8, 4529–4546, doi:10.5194/acp-8-4529-2008, 2008.
- Chen, D., Wang, Y., McElroy, M. B., He, K., Yantosca, R. M., and Le Sager, P.: Regional CO pollution and export in China simulated by the high-resolution nested-grid GEOS-Chem model, *Atmos. Chem. Phys.*, 9, 3825–3839, doi:10.5194/acp-9-3825-2009, 2009.
- Emmerson, K. M. and Evans, M. J.: Comparison of tropospheric gas-phase chemistry schemes for use within global models, *Atmos. Chem. Phys.*, 9, 1831–1845, doi:10.5194/acp-9-1831-2009, 2009.
- Evans, M. J. and Jacob, D. J.: Impact of new laboratory studies of N₂O₅ hydrolysis on global model budgets of tropospheric nitrogen oxides, ozone, and OH, *Geophys. Res. Lett.*, 32, L09813, doi:10.1029/2005gl022469, 2005.
- Fiore, A. M., Horowitz, L. W., Purves, D. W., Levy, H., Evans, M. J., Wang, Y. X., Li, Q. B., and Yantosca, R. M.: Evaluating the contribution of changes in isoprene emissions to surface ozone trends over the eastern United States, *J. Geophys. Res.-Atmos.*, 110, D12303, doi:10.1029/2004jd005485, 2005.

- Fortems-Cheiney, A., Chevallier, F., Pison, I., Bousquet, P., Szopa, S., Deeter, M. N., and Clerbaux, C.: Ten years of CO emissions as seen from Measurements of Pollution in the Troposphere (MOPITT), *J. Geophys. Res.-Atmos.*, 116, D05304, doi:10.1029/2010jd014416, 2011.
- Global Modeling and Assimilation Office: File Specification for GEOS-5 DAS Gridded Output Document No. GMAO-1001v6.1, 2006.
- He, K. B., Yang, F. M., Ma, Y. L., Zhang, Q., Yao, X. H., Chan, C. K., Cadle, S., Chan, T., and Mulawa, P.: The characteristics of PM_{2.5} in Beijing, China, *Atmos. Environ.*, 35, 4959–4970, 2001.
- Holtzlag, A. and Boville, B.: Local versus nonlocal boundary-layer diffusion in a global climate model, *J. Climate*, 6, 1825–1842, 1993.
- Hudman, R. C., Jacob, D. J., Turquety, S., Leibensperger, E. M., Murray, L. T., Wu, S., Gilliland, A. B., Avery, M., Bertram, T. H., Brune, W., Cohen, R. C., Dibb, J. E., Flocke, F. M., Fried, A., Holloway, J., Neuman, J. A., Orville, R., Perring, A., Ren, X., Sachse, G. W., Singh, H. B., Swanson, A., and Wooldridge, P. J.: Surface and lightning sources of nitrogen oxides over the United States: Magnitudes, chemical evolution, and outflow, *J. Geophys. Res.-Atmos.*, 112, D12S05, doi:10.1029/2006jd007912, 2007.
- Huijnen, V., Eskes, H. J., Poupkou, A., Elbern, H., Boersma, K. F., Foret, G., Sofiev, M., Valdebenito, A., Flemming, J., Stein, O., Gross, A., Robertson, L., D'Isidoro, M., Kioutsioukis, I., Friese, E., Amstrup, B., Bergstrom, R., Strunk, A., Vira, J., Zyryanov, D., Maurizi, A., Melas, D., Peuch, V.-H., and Zerefos, C.: Comparison of OMI NO₂ tropospheric columns with an ensemble of global and European regional air quality models, *Atmos. Chem. Phys.*, 10, 3273–3296, doi:10.5194/acp-10-3273-2010, 2010.
- Ito, A., Sillman, S., and Penner, J. E.: Global chemical transport model study of ozone response to changes in chemical kinetics and biogenic volatile organic compounds emissions due to increasing temperatures: Sensitivities to isoprene nitrate chemistry and grid resolution, *J. Geophys. Res.-Atmos.*, 114, D09301, doi:10.1029/2008jd011254, 2009.
- Jacob, D. J.: Heterogeneous chemistry and tropospheric ozone, *Atmos. Environ.*, 34, 2131–2159, doi:10.1016/s1352-2310(99)00462-8, 2000.
- Jaeglé, L., Steinberger, L., Martin, R. V., and Chance, K.: Global partitioning of NO_x sources using satellite observations: Relative roles of fossil fuel combustion, biomass burning and soil emissions, *Faraday Discuss.*, 130, 407–423, doi:10.1039/b502128f, 2005.
- Karl, T., Harley, P., Emmons, L., Thornton, B., Guenther, A., Basu, C., Turnipseed, A., and Jardine, K.: Efficient Atmospheric Cleansing of Oxidized Organic Trace Gases by Vegetation, *Science*, 330, 816–819, doi:10.1126/science.1192534, 2010.
- Kolb, C. E., Cox, R. A., Abbatt, J. P. D., Ammann, M., Davis, E. J., Donaldson, D. J., Garrett, B. C., George, C., Griffiths, P. T., Hanson, D. R., Kulmala, M., McFiggans, G., Pöschl, U., Riipinen, I., Rossi, M. J., Rudich, Y., Wagner, P. E., Winkler, P. M., Worsnop, D. R., and O' Dowd, C. D.: An overview of current issues in the uptake of atmospheric trace gases by aerosols and clouds, *Atmos. Chem. Phys.*, 10, 10561–10605, doi:10.5194/acp-10-10561-2010, 2010.
- Kubistin, D., Harder, H., Martinez, M., Rudolf, M., Sander, R., Bozem, H., Eerdeken, G., Fischer, H., Gurk, C., Klüpfel, T., Königstedt, R., Parchatka, U., Schiller, C. L., Stickler, A., Taraborrelli, D., Williams, J., and Lelieveld, J.: Hydroxyl radicals in the tropical troposphere over the Suriname rainforest: comparison of measurements with the box model MECCA, *Atmos. Chem. Phys.*, 10, 9705–9728, doi:10.5194/acp-10-9705-2010, 2010.
- Lamsal, L. N., Martin, R. V., van Donkelaar, A., Celarier, E. A., Bucsela, E. J., Boersma, K. F., Dirksen, R., Luo, C., and Wang, Y.: Indirect validation of tropospheric nitrogen dioxide retrieved from the OMI satellite instrument: Insight into the seasonal variation of nitrogen oxides at northern midlatitudes, *J. Geophys. Res.-Atmos.*, 115, D05302, doi:10.1029/2009jd013351, 2010.
- Lamsal, L. N., Martin, R. V., Padmanabhan, A., van Donkelaar, A., Zhang, Q., Sioris, C. E., Chance, K., Kurosu, T. P., and Newchurch, M. J.: Application of satellite observations for timely updates to global anthropogenic NO_x emission inventories, *Geophys. Res. Lett.*, 38, L05810, doi:10.1029/2010gl046476, 2011.
- Lelieveld, J., Butler, T. M., Crowley, J. N., Dillon, T. J., Fischer, H., Ganzeveld, L., Harder, H., Lawrence, M. G., Martinez, M., Taraborrelli, D., and Williams, J.: Atmospheric oxidation capacity sustained by a tropical forest, *Nature*, 452, 737–740, doi:10.1038/nature06870, 2008.
- Li, S., Matthews, J., and Sinha, A.: Atmospheric hydroxyl radical production from electronically excited NO₂ and H₂O, *Science*, 319, 1657–1660, doi:10.1126/science.1151443, 2008.
- Li, S., Matthews, J., and Sinha, A.: Response to Comment on “Atmospheric Hydroxyl Radical Production from Electronically Excited NO₂ and H₂O”, *Science*, 324, p. 336, doi:10.1126/science.1166877, 2009.
- Lin, J.-T.: Satellite constraint for emissions of nitrogen oxides from anthropogenic, lightning and soil sources over East China on a high-resolution grid, *Atmos. Chem. Phys.*, 12, 2881–2898, doi:10.5194/acp-12-2881-2012, 2012.
- Lin, J. T. and McElroy, M. B.: Impacts of boundary layer mixing on pollutant vertical profiles in the lower troposphere: Implications to satellite remote sensing, *Atmos. Environ.*, 44, 1726–1739, doi:10.1016/j.atmosenv.2010.02.009, 2010.
- Lin, J.-T. and McElroy, M. B.: Detection from space of a reduction in anthropogenic emissions of nitrogen oxides during the Chinese economic downturn, *Atmos. Chem. Phys.*, 11, 8171–8188, doi:10.5194/acp-11-8171-2011, 2011.
- Lin, J.-T., Liang, X.-Z., and Wuebbles, D. J.: Effects of Intercontinental Transport on Surface Ozone over the United States: Present and Future Assessment with a Global Model, *Geophys. Res. Lett.*, 35, L02805, doi:10.1029/2007GL031415, 2008a.
- Lin, J.-T., Youn, D., Liang, X.-Z., and Wuebbles, D. J.: Global model simulation of summertime U.S. ozone diurnal cycle and its sensitivity to PBL mixing, spatial resolution, and emissions, *Atmos. Environ.*, 42, 8470–8483, doi:10.1016/j.atmosenv.2008.08.012, 2008b.
- Lin, J.-T., Patten, K. O., Hayhoe, K., Liang, X.-Z., and Wuebbles, D. J.: Effects of future climate and biogenic emission changes on surface ozone over the United States and China, *J. Appl. Meteor.*, 47, 1888–1909, doi:10.1175/2007JAMC1681.1, 2008c.
- Lin, J., Nielsen, C. P., Zhao, Y., Lei, Y., Liu, Y., and McElroy, M. B.: Recent Changes in Particulate Air Pollution over China Observed from Space and the Ground: Effectiveness of Emission Control, *Environ. Sci. Technol.*, 44, 7771–7776, doi:10.1021/es101094t, 2010a.

- Lin, J.-T., McElroy, M. B., and Boersma, K. F.: Constraint of anthropogenic NO_x emissions in China from different sectors: a new methodology using multiple satellite retrievals, *Atmos. Chem. Phys.*, 10, 63–78, doi:10.5194/acp-10-63-2010, 2010b.
- Liu, H., Crawford, J. H., Considine, D. B., Platnick, S., Norris, P. M., Duncan, B. N., Pierce, R. B., Gao, C., and Yantosca, R. M.: Sensitivity of photolysis frequencies and key tropospheric oxidants in a global model to cloud vertical distributions and optical properties, *J. Geophys. Res.*, 114, D10305, doi:10.1029/2008jd011503, 2009.
- Liu, S. and Liang, X.-Z.: Observed Diurnal Cycle Climatology of Planetary Boundary Layer Height, *J. Climate*, 23, 5790–5809, doi:10.1175/2010jcli3552.1, 2010.
- Liu, Z., Wang, Y., Gu, D., Zhao, C., Huey, L. G., Stickel, R., Liao, J., Shao, M., Zhu, T., Zeng, L., Liu, S.-C., Chang, C.-C., Amoroso, A., and Costabile, F.: Evidence of Reactive Aromatics As a Major Source of Peroxy Acetyl Nitrate over China, *Environ. Sci. Technol.*, 44, 7017–7022, doi:10.1021/es1007966, 2010.
- Liu, Z., Wang, Y., Zhao, C., Vrekoussis, M., Richter, A., Wittrock, F., Burrow, J. P., Shao, M., Liu, S.-C., Chang, C.-C., Wang, H., and Chen, C.: The Missing Source of Glyoxal over China and Its Implications on Organic Aerosol Budgets, *American Geophysical Union Fall Meeting 2011*, San Francisco, 2011.
- Liu, Z., Wang, Y., Gu, D., Zhao, C., Huey, L. G., Stickel, R., Liao, J., Shao, M., Zhu, T., Zeng, L., Amoroso, A., Costabile, F., Chang, C.-C., and Liu, S.-C.: Summertime photochemistry during CAREBeijing-2007: RO_x budgets and O₃ formation, *Atmos. Chem. Phys.*, 12, 7737–7752, doi:10.5194/acp-12-7737-2012, 2012.
- Lu, Z., Zhang, Q., and Streets, D. G.: Sulfur dioxide and primary carbonaceous aerosol emissions in China and India, 1996–2010, *Atmos. Chem. Phys.*, 11, 9839–9864, doi:10.5194/acp-11-9839-2011, 2011.
- Macintyre, H. L. and Evans, M. J.: Parameterisation and impact of aerosol uptake of HO₂ on a global tropospheric model, *Atmos. Chem. Phys.*, 11, 10965–10974, doi:10.5194/acp-11-10965-2011, 2011.
- Mao, J., Jacob, D. J., Evans, M. J., Olson, J. R., Ren, X., Brune, W. H., St. Clair, J. M., Crounse, J. D., Spencer, K. M., Beaver, M. R., Wennberg, P. O., Cubison, M. J., Jimenez, J. L., Fried, A., Weibring, P., Walega, J. G., Hall, S. R., Weinheimer, A. J., Cohen, R. C., Chen, G., Crawford, J. H., Jaeglé, L., Fisher, J. A., Yantosca, R. M., Le Sager, P., and Carouge, C.: Chemistry of hydrogen oxide radicals (HO_x) in the Arctic troposphere in spring, *Atmos. Chem. Phys.*, 10, 5823–5838, doi:10.5194/acp-10-5823-2010, 2010.
- Mao, J., Fan S., and Jacob, D. J.: Radical loss in the atmosphere from Cu-Fe redox coupling in aerosols, *Nature*, in review, 2012.
- Martin, R. V., Jacob, D. J., Chance, K., Kurosu, T. P., Palmer, P. I., and Evans, M. J.: Global inventory of nitrogen oxide emissions constrained by space-based observations of NO₂ columns, *J. Geophys. Res.*, 108, 4537, doi:10.1029/2003JD003453, 2003.
- Martin, R. V., Sioris, C. E., Chance, K., Ryerson, T. B., Bertram, T. H., Wooldridge, P. J., Cohen, R. C., Neuman, J. A., Swanson, A., and Flocke, F. M.: Evaluation of space-based constraints on global nitrogen oxide emissions with regional aircraft measurements over and downwind of eastern North America, *J. Geophys. Res.*, 111, D15308, doi:10.1029/2005JD006680, 2006.
- Mijling, B., van der A, R. J., Boersma, K. F., Van Roozendaal, M., De Smedt, I., and Kelder, H. M.: Reductions of NO₂ detected from space during the 2008 Beijing Olympic Games, *Geophys. Res. Lett.*, 36, D13801, doi:10.1029/2009gl038943, 2009.
- Mollner, A. K., Valluvadasan, S., Feng, L., Sprague, M. K., Okumura, M., Milligan, D. B., Bloss, W. J., Sander, S. P., Martien, P. T., Harley, R. A., McCoy, A. B., and Carter, W. P. L.: Rate of Gas Phase Association of Hydroxyl Radical and Nitrogen Dioxide, *Science*, 330, 646–649, doi:10.1126/science.1193030, 2010.
- Okumura, M. and Sander, S. P.: Gas-Phase Formation Rates of Nitric Acid and its Isomers under Urban Conditions, *State of California Air Resources Board*, 2005.
- Patchen, A. K., Pennino, M. J., Kiep, A. C., and Elrod, M. J.: Direct kinetics study of the product-forming channels of the reaction of isoprene-derived hydroxyperoxy radicals with NO, *Int. J. Chem. Kinet.*, 39, 353–361, doi:10.1002/kin.20248, 2007.
- Paulot, F., Crounse, J. D., Kjaergaard, H. G., Kroll, J. H., Seinfeld, J. H., and Wennberg, P. O.: Isoprene photooxidation: new insights into the production of acids and organic nitrates, *Atmos. Chem. Phys.*, 9, 1479–1501, doi:10.5194/acp-9-1479-2009, 2009.
- Pryor, S. C. and Barthelmie, R. J.: Assessing climate change impacts on the near-term stability of the wind energy resource over the United States, *P. Natl. Acad. Sci. USA*, 108, 8167–8171, doi:10.1073/pnas.1019388108, 2011.
- Richter, A., Burrows, J. P., Nüß, H., Granier, C., and Niemeier, U.: Increase in tropospheric nitrogen dioxide over China observed from space, *Nature*, 437, 129–132, doi:10.1038/nature04092, 2005.
- Sander, S. P., Abbatt, J. P. D., Barker, J. R., Burkholder, J. B., Friedl, R. R., Golden, D. M., Huie, R. E., Kolb, C. E., Kurylo, M. J., Moortgat, G. K., Orkin, V. L., and Wine, P. H.: *Chemical Kinetics and Photochemical Data for Use in Atmospheric Studies*, Pasadena, JPL Publication 10-06, 2011.
- Saunders, S. M., Jenkin, M. E., Derwent, R. G., and Pilling, M. J.: Protocol for the development of the Master Chemical Mechanism, MCM v3 (Part A): tropospheric degradation of non-aromatic volatile organic compounds, *Atmos. Chem. Phys.*, 3, 161–180, doi:10.5194/acp-3-161-2003, 2003.
- Sauvage, B., Martin, R. V., van Donkelaar, A., Liu, X., Chance, K., Jaeglé, L., Palmer, P. I., Wu, S., and Fu, T.-M.: Remote sensed and in situ constraints on processes affecting tropical tropospheric ozone, *Atmos. Chem. Phys.*, 7, 815–838, doi:10.5194/acp-7-815-2007, 2007.
- Stavrakou, T., Muller, J. F., Boersma, K. F., De Smedt, I., and van der A, R. J.: Assessing the distribution and growth rates of NO_x emission sources by inverting a 10-year record of NO₂ satellite columns, *Geophys. Res. Lett.*, 35, L10801, doi:10.1029/2008gl033521, 2008.
- Streets, D. G., Bond, T. C., Carmichael, G. R., Fernandes, S. D., Fu, Q., He, D., Klimont, Z., Nelson, S. M., Tsai, N. Y., Wang, M. Q., Woo, J. H., and Yarber, K. F.: An inventory of gaseous and primary aerosol emissions in Asia in the year 2000, *J. Geophys. Res.-Atmos.*, 108, 8809, doi:10.1029/2002jd003093, 2003.
- Su, H., Cheng, Y. F., Oswald, R., Behrendt, T., Trebs, I., Meixner, F. X., Andreae, M. O., Cheng, P., Zhang, Y., and Pöschl, U.: Soil Nitrite as a Source of Atmospheric HONO and OH Radicals, *Science*, 333, 1616–1618, doi:10.1126/science.1207687, 2011.
- Taketani, F., Kanaya, Y., Pochanart, P., Liu, Y., Li, J., Okuzawa, K., Kawamura, K., Wang, Z., and Akimoto, H.: Measurement

- of overall uptake coefficients for HO₂ radicals by aerosol particles sampled from ambient air at Mts. Tai and Mang (China), *Atmos. Chem. Phys.*, 12, 11907–11916, doi:10.5194/acp-12-11907-2012, 2012.
- Thornton, J. A., Jaeglé, L., and McNeill, V. F.: Assessing known pathways for HO₂ loss in aqueous atmospheric aerosols: Regional and global impacts on tropospheric oxidants, *J. Geophys. Res.-Atmos.*, 113, D05303, doi:10.1029/2007jd009236, 2008.
- Tost, H., Lawrence, M. G., Brühl, C., Jöckel, P., The GABRIEL Team, and The SCOUT-O₃-DARWIN/ACTIVE Team: Uncertainties in atmospheric chemistry modelling due to convection parameterisations and subsequent scavenging, *Atmos. Chem. Phys.*, 10, 1931–1951, doi:10.5194/acp-10-1931-2010, 2010.
- Valin, L. C., Russell, A. R., Hudman, R. C., and Cohen, R. C.: Effects of model resolution on the interpretation of satellite NO₂ observations, *Atmos. Chem. Phys.*, 11, 11647–11655, doi:10.5194/acp-11-11647-2011, 2011.
- van der A, R. J., Peters, D., Eskes, H., Boersma, K. F., Van Roozendael, M., De Smedt, I., and Kelder, H. M.: Detection of the trend and seasonal variation in tropospheric NO₂ over China, *J. Geophys. Res.-Atmos.*, 111, D12317, doi:10.1029/2005jd006594, 2006.
- van Noije, T. P. C., Eskes, H. J., Dentener, F. J., Stevenson, D. S., Ellingsen, K., Schultz, M. G., Wild, O., Amann, M., Atherton, C. S., Bergmann, D. J., Bey, I., Boersma, K. F., Butler, T., Co-fala, J., Drevet, J., Fiore, A. M., Gauss, M., Hauglustaine, D. A., Horowitz, L. W., Isaksen, I. S. A., Krol, M. C., Lamarque, J.-F., Lawrence, M. G., Martin, R. V., Montanaro, V., Müller, J.-F., Pitari, G., Prather, M. J., Pyle, J. A., Richter, A., Rodriguez, J. M., Savage, N. H., Strahan, S. E., Sudo, K., Szopa, S., and van Roozendael, M.: Multi-model ensemble simulations of tropospheric NO₂ compared with GOME retrievals for the year 2000, *Atmos. Chem. Phys.*, 6, 2943–2979, doi:10.5194/acp-6-2943-2006, 2006.
- Wang, S. W., Zhang, Q., Streets, D. G., He, K. B., Martin, R. V., Lamsal, L. N., Chen, D., Lei, Y., and Lu, Z.: Growth in NO_x emissions from power plants in China: bottom-up estimates and satellite observations, *Atmos. Chem. Phys.*, 12, 4429–4447, doi:10.5194/acp-12-4429-2012, 2012.
- Wu, S., Mickley, L. J., Jacob, D. J., Logan, J. A., Yantosca, R. M., and Rind, D.: Why are there large differences between models in global budgets of tropospheric ozone?, *J. Geophys. Res.-Atmos.*, 112, D05302, doi:10.1029/2006jd007801, 2007.
- Yang, F., Tan, J., Zhao, Q., Du, Z., He, K., Ma, Y., Duan, F., Chen, G., and Zhao, Q.: Characteristics of PM_{2.5} speciation in representative megacities and across China, *Atmos. Chem. Phys.*, 11, 5207–5219, doi:10.5194/acp-11-5207-2011, 2011.
- Zhang, Q., Streets, D. G., He, K., Wang, Y., Richter, A., Burrows, J. P., Uno, I., Jang, C. J., Chen, D., Yao, Z., and Lei, Y.: NO_x emission trends for China, 1995–2004: The view from the ground and the view from space, *J. Geophys. Res.*, 112, D22306, doi:10.1029/2007JD008684, 2007.
- Zhang, L., Jacob, D. J., Boersma, K. F., Jaffe, D. A., Olson, J. R., Bowman, K. W., Worden, J. R., Thompson, A. M., Avery, M. A., Cohen, R. C., Dibb, J. E., Flock, F. M., Fuelberg, H. E., Huey, L. G., McMillan, W. W., Singh, H. B., and Weinheimer, A. J.: Transpacific transport of ozone pollution and the effect of recent Asian emission increases on air quality in North America: an integrated analysis using satellite, aircraft, ozonesonde, and surface observations, *Atmos. Chem. Phys.*, 8, 6117–6136, doi:10.5194/acp-8-6117-2008, 2008.
- Zhang, Q., Streets, D. G., and He, K. B.: Satellite observations of recent power plant construction in Inner Mongolia, China, *Geophys. Res. Lett.*, 36, L15809, doi:10.1029/2009gl038984, 2009a.
- Zhang, Q., Streets, D. G., Carmichael, G. R., He, K. B., Huo, H., Kannari, A., Klimont, Z., Park, I. S., Reddy, S., Fu, J. S., Chen, D., Duan, L., Lei, Y., Wang, L. T., and Yao, Z. L.: Asian emissions in 2006 for the NASA INTEX-B mission, *Atmos. Chem. Phys.*, 9, 5131–5153, doi:10.5194/acp-9-5131-2009, 2009b.
- Zhao, C. and Wang, Y. H.: Assimilated inversion of NO_x emissions over east Asia using OMI NO₂ column measurements, *Geophys. Res. Lett.*, 36, L06805, doi:10.1029/2008gl037123, 2009.